uOttawa

L'Université canadienne
Canada's university

FACULTÉ DES ÉTUDES SUPÉRIEURES ET POSTOCTORALES

uOttawa

L'Université canadienne
Canada's university

FACULTY OF GRADUATE AND POSDOCTORAL STUDIES

Hooman Ghassemi

AUTEUR DE LA THÈSE / AUTHOR OF THESIS

M.A.Sc. (Environmental Engineering)

GRADE / DEGREE

Program of Environmental Engineering

FACULTÉ, ÉCOLE, DÉPARTEMENT / FACULTY, SCHOOL, DEPARTMENT

Impacts of Biofilm on Diffusion in Fractured Rock

TITRE DE LA THÈSE / TITLE OF THESIS

Dr. Nathalie Rossi

DIRECTEUR (DIRECTRICE) DE LA THÈSE / THESIS SUPERVISOR

Dr. Paul Van Geel

CO-DIRECTEUR (CO-DIRECTRICE) DE LA THÈSE / THESIS CO-SUPERVISOR

EXAMINATEURS (EXAMINATRICES) DE LA THÈSE / THESIS EXAMINERS

Dr. D. Karman

Dr. K. Kennedy

Dr. J. Zhang

Gary W. Slater

Le Doyen de la Faculté des études supérieures et postdoctorales / Dean of the Faculty of Graduate and Postdoctoral Studies

IMPACTS OF BIOFILM ON DIFFUSION IN FRACTURED ROCK

by

Hooman Ghassemi

Thesis submitted to the Faculty of Graduate and Postdoctoral Studies

In partial fulfillment of the requirements for the degree of

Master of Applied Science in Environmental Engineering

The Ottawa-Carleton Institute for Environmental Engineering

University of Ottawa

Your file Votre référence
ISBN: 978-0-494-32449-3
Our file Notre référence
ISBN: 978-0-494-32449-3

ABSTRACT

Fractured rock aquifers consist of complex flow systems that impose several constraints on cleanup efforts. Remedial techniques in such aquifers are influenced by diffusion of contaminants into the rock matrix and the subsequent back diffusion into the fracture. In particular, the back diffusion process can release a low concentration of contaminant into the groundwater for an extended period of time after the main source of contamination is removed from the fracture network.

Biofilms have been defined as cells immobilized on a solid surface and embedded in a gel matrix of extra-cellular polymeric substances (EPS) excreted by microorganisms. Biofilms can be stimulated on rock surfaces to act as a barrier in groundwater systems, which influences hydraulic properties of the fractured media as well as the rate of contaminant transport between the rock matrix and the fracture.

The main objective of this study was to assess the potential of a biofilm to limit diffusion between the host rock and fracture. The impacts of different types of microorganisms on the diffusion rate were compared, and the performances of the tracers employed in diffusion experiments were evaluated. *P. putida*, *E. coli* and an indigenous groundwater population were used to grow biofilm on porous ceramic disks with nominal pore diameter of 6 μm. Disks were installed into stainless steel double-reservoir cells. The source reservoirs were spiked to obtain initial concentrations of 1500 ppm of bromide and 5000 ppb of Lissamine. In total, 17 experiments were conducted to assess the diffusion. Finally,

a semi analytical model was used to interpret the geometric factors (tortuosity) of the porous media and the impacts of the biofilm on the effective diffusion coefficient.

Results, estimated from bromide and Lissamine concentration profiles, did not suggest a significant impact of biofilm on the diffusion through the ceramic disks. This could be due to heterogeneity of biofilm structures, loose structures of developed biofilms, lack of biofilm penetration into the pores inside the disks as a result of nutrient overloading or biofilm decay/detachment during the test. In addition, Lissamine did not appear to perform as a conservative tracer in some cases where mass balance calculations indicated a loss of dye.

It was recommended to characterize the biofilm structure as well as the biofilm impregnated zone, and to adjust the nutrient loading in order to obtain a more packed structure for the biofilm developed by small size bacteria. Recommendations also included a thorough evaluation of Lissamine behaviour as a conservative tracer.

ACKNOWLEDGEMENTS

Program for Energy Research and Development (PERD) provided financial support for this research.

I would like to thank my supervisors, Nathalie Ross and Paul Van Geel, for their patient supervision, endless care and advice that I needed to complete this thesis.

Thank you to Kent Novakowski and Grace Yungwirth for giving their superb and creative suggestions and for sharing the FORTRAN code of the mathematical model.

Special thanks to Louis Tremblay and Franco Ziroldo for their excellent technical support and their effort on making the experimental cells.

Thanks to Patrick Juneau and Deepak Sharma for their interest, feedback and advice on microbiology aspect of this project.

I would also like to thank those friends who made the whole experience enjoyable. To Arturo Macchi, thank you for his continuous care and support, and to Suzanne Labelle, a huge thank you for all the cheerful moments.

Lastly, thanks to my wife, Shahrzad, and to my parents, for all their love and devotion.

FOREWORD

This document complies with the requirements for a manuscript format thesis. Chapter 1 provides an introduction and consists of a description of the scope of this project. Chapter 2 is a review of the available literature on the subject. Chapter 3 presents the results in manuscript format. In chapter 4, general conclusions and recommendations for future works on the subject are presented. All auxiliary information is presented in appendices. Hooman Ghassemi is the primary author of the entire document.

TABLE OF CONTENT

LIST OF TABLES

LIST OF FIGURES

NOMENCLATURE

A	cross-sectional area of the porous media [L^2]
C	solute concentration [$M\ L^{-3}$]
C_0	initial solute concentration [$M\ L^{-3}$]
C_e	solute concentrations in exit reservoir [$M\ L^{-3}$]
C_s	solute concentrations in source reservoir [$M\ L^{-3}$]
D^*	effective diffusion coefficient [$L^2\ T^{-1}$]
D_0	free aqueous diffusion coefficient [$L^2\ T^{-1}$]
D_h	hydrodynamic dispersion coefficient [$L^2\ T^{-1}$]
D_m	mechanical dispersion coefficient [$L^2\ T^{-1}$]
J	mass flux [$M\ L^{-2}\ T^{-1}$]
J_D	diffusive mass flux [$M\ L^{-2}\ T^{-1}$]
L	porous disk thickness [L]
L_e	equivalent length of the solute transport path [L]
L_E	length of the exit reservoir [L]
L_P	length of the porous zone [L]
L_S	length of the source reservoir [L]
L_t	total length of the solute transport path [L]
m	solute mass [M]
M.B.	mass balance
n	total porosity
n_d	storage porosity
n_t	transport or effective porosity

R	chemical or biological reactions rate [M L^{-3} T^{-1}]
R_d	retardation factor
s	Laplace variable
t	time [T]
V_d	volume of the porous disk [L^3]
V_e	volume of exit reservoir [L^3]
V_s	volume of source reservoir [L^3]
v_s	seepage velocity [L T^{-1}]
x	direction of the transport [L]
γ	effective cross sectional area [L^2]
Δ	divergence operator
λ	decay rate constant [T^{-1}]
τ	tortuosity factor

1 INTRODUCTION

Uncontrolled releases of contaminants into groundwater resources during the past decades have resulted in serious health problems. The increasing demand for drinking water and the finite nature of our groundwater resources, on the other hand, have highlighted the need for cleanup of contaminated groundwater resources. It is the reason why over the past two decades, extensive attention has been devoted to develop appropriate remedial techniques for polluted sites.

Dense non-aqueous phase liquids (DNAPLs) are a major source of groundwater contamination. DNAPLs are generally characterized by a combination of high density, low viscosity and relatively low solubility in water. These liquids can migrate downward as a separate phase through both saturated and unsaturated zones, leaving a trail of liquid at residual saturation (VanderKwaak and Sudicky, 1996). In fractured geological media (Fig. 1.1), DNAPL preferentially migrates along the fracture and also enters the rock matrix (Kueper and McWhorter, 1991). The transfer of the aqueous phase contaminant between the fracture and rock matrix is due to a concentration gradient and is governed by the diffusion mechanism. The DNAPL's aqueous components adsorbed to the rock matrix can act as a persistent source of contamination by desorbing into the groundwater flow for an extended period of time after the source of contamination is removed by hydrodynamic forces (Mutch et al., 1993). This phenomenon, referred to as back diffusion, is also due to a concentration gradient between the rock matrix and discrete fracture (Fig. 1.2). Although sparingly soluble in many cases, DNAPL solubility often exceeds drinking water standards by orders of magnitude (e.g. Ministry of Environment, 2003).

Conventional remedial techniques can be very costly and, in some cases, impractical when the target zone is a complex formation such as fractured rock. Such conventional techniques may necessitate tremendous amounts of excavation, pumpage and treatment in a complex and sometimes uncharacterized site. Biological remediation techniques, also referred to as bioremediation techniques, on the other hand, have offered remarkable benefits in cleanup of fractured rock aquifers. Bioremediation technologies include a variety of techniques in which the microorganisms are exploited to degrade the contaminants, or to block the contaminated zones (Ross and Bickerton, 2002).

Biofilms are microbial systems that form when bacteria attach to surfaces in aqueous environments and begin to excrete glue-like polymeric substances. Biofilms have been employed as biobarriers to clog pores and fractures in sub-surface environments, in order to control the groundwater movement and contaminant transport (Ross and Bickerton, 2002; Johnston et al., 1999). Several laboratory experiments have proven a significant reduction of hydraulic conductivity of porous media due to bioclogging (Cunningham et al., 1991; Taylor and Jaffé, 1990; Shaw et al., 1985). Field studies have also been carried out to investigate the potential for groundwater containment by stimulating the indigenous population of microorganisms to form a biobarrier (Cunningham et al., 2003). More recently, a number of laboratory and field studies have been undertaken in which the potential of bioclogging in fractured media has been investigated (Ross et al., 2001; Ross and Bickerton, 2002; Hill and Sleep, 2002). Several models have also been introduced to simulate the observed interactions between biomass and the hydraulic properties of porous

media. Usually, these models are based on the assumption of a homogeneous biofilm covering the surface of the grains (Taylor et al., 1990; Thullner et al., 2002).

Biofilm development on the rock surface may also limit the contaminant transport between the rock matrix and fracture. Biofilm can impact the diffusion rate of a contaminant into the rock matrix. It can potentially limit the back diffusion of a contaminant into the fracture as well. This containment mechanism has been examined in the most recent studies on the subject (Charbonneau et al., 2006).

The objective of this study, in general, was to assess the potential of biofilm to reduce diffusion between the host rock and fracture. The performances of different microorganisms exploited to develop a biofilm were compared as well. In order to address these questions, a set of diffusion experiments were carried out using double-reservoir cells. Two types of tracer (bromide and Lissamine) were used in the diffusion experiments and the impacts of three types of biofilm (developed from two pure cultures and one indigenous population) were compared. The performance of Lissamine as a conservative tracer was also evaluated. A conceptual model was developed to assist in experiment design. By fitting the model to experimental results, it was possible to estimate the model parameters. The experimental results were also used to validate the model.

This thesis includes four chapters. Followed by this chapter, there is a literature review that is divided into two major categories: 1- Basic concept of a biofilm, its components, structure and application, 2- Diffusion principles. In chapter three, presented in manuscript format, the effects of biofilm on diffusion between the rock matrix and a discrete fracture

are discussed. The mathematical model, used to simulate the diffusion between a rock matrix and fracture reservoir, is presented in this chapter. In addition, the experimental approach, methods and material used, as well as the experimental data obtained from the diffusion cells are included in chapter three. Lastly, conclusions and recommendations for future works are mentioned in chapter four. Auxiliary information is also presented in the appendices.

1.1 References

Charbonneau, A., Novakowski, K., Ross, N. 2006. The effect of a biofilm on solute diffusion in fractured porous media. Journal of Contaminant Hydrology 85: 212–228.

Cunningham, A.B., Characklis, W.G., Abedeen, F., Crawford, D. 1991. Influence of biofilm accumulation on porous media hydrodynamics. Environmental Science and Technology 25: 1305-1311.

Cunningham, A.B., Sharp, R.R., Hiebert, R., James, G. 2003. Subsurface biofilm barriers for the containment and remediation of contaminated groundwater. Bioremediation Journal 7(3-4): 151-164.

Hill, D.H., Sleep, B.E. 2002. Effects of biofilm growth on flow and transport through a glass parallel plate fracture. Journal of Contaminant Hydrology 56: 227-246.

Johnston, C.D., Trefry, M.G., Rayner, J.L., Ragusa, S.R., De Zoysa, D.S., Davis, G.B. 1999. In situ bioclogging for the confinement and remediation of groundwater hydrocarbon plumes. Contaminated Site Remediation Conference, Fremantle, Western Australia.

Kueper, B.H., McWhorter, D.B. 1991. The behavior of dense, non-aqueous-phase liquids in fractured clay and rock. Ground Water 29(5): 716-728.

Ministry of Environment, Government of Ontario. 2003. Technical support document for Ontario drinking water standards, objectives and guidelines.

Mutch, R.D., Scott, J.I., Wilson, D.J. 1993. Cleanup of fractured rock aquifers: implications of matrix diffusion. Environmental Monitoring and Assessment 24: 45-70.

Ross, N., Bickerton, G. 2002. Application of biobarriers for groundwater containment at fractured bedrock sites. Remediation 12 (3): 5-21.

Ross, N., Villemur, R., Deschênes, L., Samson, R. 2001. Clogging of a limestone fracture by stimulating groundwater microbes. Water Research 35: 2029-2037.

Shaw, J.C., Bramhill, B., Wardlaw, N.C., Costerton, J.W. 1985. Bacterial fouling in a model core system. Applied and Environmental Microbiology 49: 693-701.

Taylor, S.W., Jaffé, P.R. 1990. Biofilm growth and the related changes in the physical properties of a porous medium, 1. Experimental investigation. Water Resources Research 26(9): 2153-2159.

Taylor, S.W., Milly, P.C.D., Jaffé, P.R. 1990. Biofilm growth and the related changes in the physical properties of a porous medium. 2. Permeability. Water Resources Research 26(9): 2161-2169.

Thullner, M., Zeyer, J., Kinzelbach, W. 2002. Influence of microbial growth on hydraulic properties of pore networks. Transport in Porous Media 49: 99-122.

VanderKwaak, J.E., Sudicky, E.A. 1996. Dissolution of non-aqueous-phase liquids and aqueous-phase contaminant transport in discretely-fractured porous media. Journal of Contaminant Hydrology 23: 45-68.

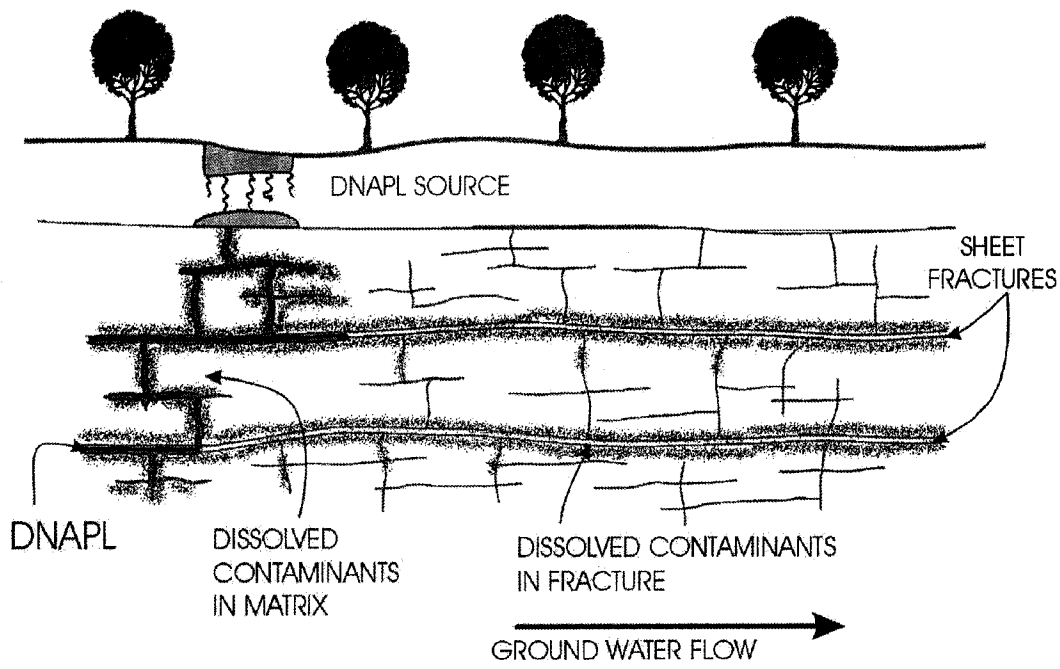

Figure 1.1: Contamination of a fractured aquifer by DNAPL (Adopted from Charbonneau, 2004).

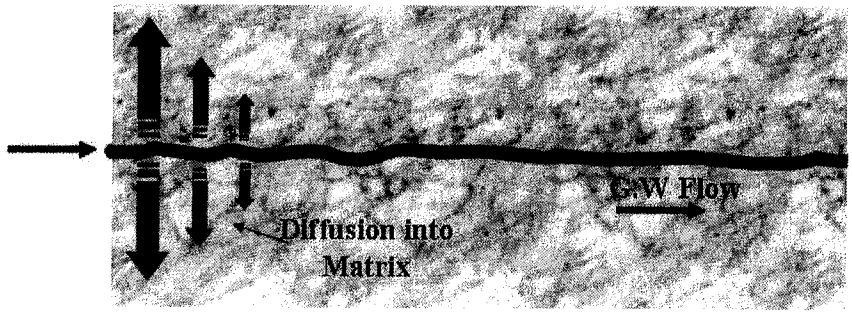

(a)

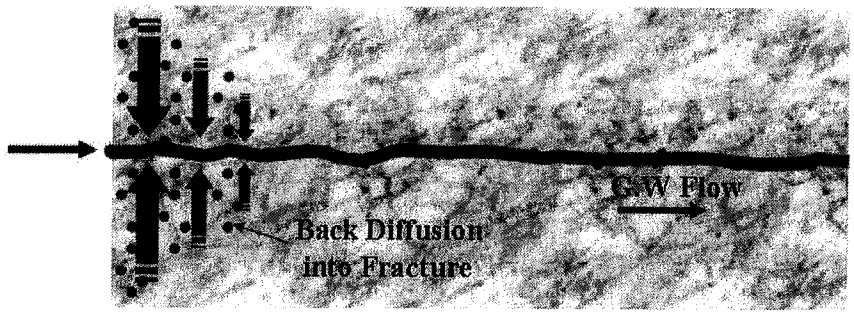

(b)

Figure 1.2: (a) Contaminant diffusion from fracture into matrix. (b) Back diffusion of contaminant into fracture.

2 LITERATURE REVIEW

2.1 Biofilms

2.1.1 Biofilm definition

Biofilms have been defined in various ways by various researchers. A consensus of the leaders in biofilm research in 1984 termed a biofilm as a collection of microorganisms, predominantly bacteria, enmeshed within a three dimensional gelatinous matrix of extracellular polymers secreted by the microorganisms (Marshall, 1984). In the first edition of *Biofilms,* Characklis and Marshall (1990) define a biofilm as consisting of "cells immobilized at a substratum and frequently embedded in an organic polymer matrix of microbial origin". A broader definition is supplied by Costerton et al. (1995) who defined biofilms as a "matrix-enclosed bacterial population adherent to each other and/or to surfaces or interfaces". Biofilms usually develop in aqueous environments. A biofilm can be formed by a single bacterial species, but more often biofilms consist of many species of bacteria, as well as fungi, algae, protozoa, debris and corrosion products. Essentially, biofilm may form on any surface exposed to bacteria and some amount of water. Once anchored to a surface, biofilm microorganisms carry out a variety of detrimental or beneficial reactions depending on the surrounding environmental conditions.

2.1.2 Biofilm composition

Besides water, biofilms are composed of two main components: the microbial communities and the extra-cellular polymeric substances (EPS) (Ross and Bickerton, 2002). Attachment to a surface is thought to initiate a cascade of physiological changes in the cell, which

leads, in part, to the overproduction of EPS (Alison and Sutherland, 1987). EPS is an open porous matrix composed of a combination of polymeric materials, including lipids, proteins, polysaccharides, polyphenols, nucleic acids and humic materials. Living microorganisms, as well as a significant fraction of inorganic or abiotic substances, become embedded within the EPS matrix. This matrix not only immobilizes the cells on the colonized surface, but also facilitates the spatial arrangement of the different species within a biofilm. Such interactions give the biofilm metabolic and physiological capabilities which are not possible for planktonic cells (Gilbert et al., 1997). EPS in biofilms formed in natural conditions may include particulate matters (clays, organic debris, phages, lysed cells, or precipitated minerals) and dissolved constituents such as nutrients, cations, and trace metals. The voids, in EPS porous matrix, are usually filled with water and soluble species which move freely through the system, primarily, by molecular diffusion (Characklis and Wilderer, 1989).

EPS was thought in the past to consist, mainly, of polysaccharides, and many detection techniques have focused on this group of compounds (e.g. Christensen and Characklis, 1990). However, recent analyses showed that EPS consists of a mixture of protein, polysaccharides, lipids and nucleic acids (Nielsen et al., 1997; Frolund et al., 1996). Protein appeared the most abundant EPS component (50% or more) in activated sludge (Frolund et al., 1996) and biofilms (Jahn and Nielsen, 1995), while polysaccharides were much less in quantity (5-20%). The actual chemical composition of non-purified EPS as it exists in natural microbial communities is largely unknown.

2.1.3 Biofilm structure

Many researchers have tried to quantify the biofilm structure as it affects the rate of nutrient transport to the deeper layers of biofilms and, ultimately, controls microbial activity and the rate of biofilm accumulation. Detailed studies have since documented that biofilm structure determines the mass transport mechanism near and within biofilms (Lawrence et al., 1991; Caldwell et al., 1992; deBeer et al., 1994; Bishop and Rittmann, 1995; Bishop, 1997).

Biofilms have a stratified structure usually involving up to five layers: the substratum, base film, surface film, bulk liquid, and gas phase (Charaklis and Marshall, 1990). Substratum is a solid phase to which microorganisms attach during early stages of accumulation. This layer may serve as the substrate as well, and its morphology may influence the rate of cell accumulation and initial population distribution. Substratum is overlain by the base film, which is a structured accumulation of microorganisms with well defined boundaries. Molecular diffusion governs the mass transport through this layer. The surface film is a transition phase between the base film and the bulk liquid. Accumulation is dominated by attachment of planktonic bacteria in this zone. The bulk liquid is a continuous liquid phase which contains both dissolved and suspended particles. The bulk liquid flows through the surface film, and also fills the pores. Lastly, a biofilm may contain a gas phase above the bulk liquid, which provides aeration and can aid in removing gaseous products from microbial reaction. It is assumed that substrates, inhibitors and electron acceptors diffuse from the bulk liquid through a liquid boundary layer at the surface film, and are utilized by the cells in the base film. There is also a counter-diffusion of the products of reaction out of biofilm. Biofilm diffusion is influenced by film density, age, thickness, porosity, presence

of filamentous organisms, microbial speciation, and electrostatic interactions (Charaklis and Marshall, 1990).

Many researchers have implicated the stratified model in their mathematical modeling of biofilm development, although there are some minor differences. Cooke et al. (1999), for example, developed a numerical model to predict the anaerobic growth of biofilm and precipitation of minerals in a granular media. Their structural model was composed of attachment area (substratum), inactive film, active biofilm, diffusion layer and bulk fluid.

Biofilms have heterogeneous structures which vary with time. The heterogeneities can be due to the polysaccharide material surrounding the bacterial clusters, pores formed after gas releases, and incomplete filling of intracluster areas. However, Bishop (1997) believes that these heterogeneities are of relatively small scale and biofilm properties can be assumed constant with depth. Several researchers, on the other hand, have suggested that the microbial species and density, pore sizes and distribution, and the tortuosity of the biofilm have to change as the depth of the biofilm increases. These spatial distributions, in turn, affect the mass transfer mechanism and diffusivities in biofilms (Zhang and Bishop, 1994).

Lastly, the hydrodynamics of the flow, in particular, the shear forces applied to a developing biofilm, as well as the substrate loading rate may affect the biofilm density. Leon Ohl et al (2004) showed that the biofilm density decreased with decreasing flow velocity in the bulk phase, while the thickness of the surface boundary layer increased. On the other hand, increasing the flow velocity in the bulk phase can lead both to a higher biofilm density and a higher maximum substrate flux. In addition, the biofilm surface

becomes more homogenous and its thickness decreases (Leon Ohl et al., 2004; Grimm et al., 2005).

2.1.4 Biofilm development

Biofilm development is a sequence of well-regulated steps which can be different from organism to organism, but the whole scenario of biofilm development is similar across a wide range of microorganisms (O'Toole, 2003). The sequential stages of biofilm development are assumed to be the results of several different processes: sorption/desorption, attachment/detachment, growth/decay, and infiltration of biomass (Cunningham, 1989).

In aqueous environments, microorganisms are subject to sorption to solid surfaces and particles due to convection, diffusion, interception and sedimentation (Schafer et al., 1998). The sorption of bacteria to solid surfaces can be predicted by the DLVO theory of colloid stability (Derjaguin and Landau, 1941; Verwey and Overbeek, 1948). This theory describes the interaction between the negatively charged bacteria and/or extracellular polymeric substances (EPS) and negatively charged solid surfaces as a sum of attractive Van der Waals forces and repulsive electrostatic forces. Hydrophobic interactions between bacteria and surfaces can also influence sorption. Basically, the sum of these interactions can explain sorption of bacteria to solid surfaces (Schafer et al., 1998). Bacteria may adsorb to surfaces due to chemical interactions as well. Chemical bonds formed in this condition have higher heats of adsorption, hence this type of sorption is usually assumed to be irreversible.

After sorption to a surface, bacteria undergo further adaptation to life in a biofilm. Surface-attached bacteria begin to synthesize EPS and develop antibiotic resistance. In a biofilm, bacteria may also develop other properties, including increased resistance to UV light, increased rates of genetic exchange, altered biodegradative capabilities, and increased secondary metabolite production (Marshall, 1992). Attachment and detachment are terms that apply at this stage. Attachment is a process by which cells are captured by the biofilm. Conversely, detachment is the transfer of the cells from the biofilm into the bulk liquid as a result of physical, chemical, or biological processes. Starvation, for example, may be a reason for detachment although this has not been investigated in detail. Boyd and Chakrabarty (1994) reported that the enzyme alginate lyase may play a role in the detachment phase in *P. aeruginosa*. They showed that over expression of alginate lyase could speed detachment from biofilms.

Processes governing biofilm formation and persistence include (Bryers, 2000):

1) Accumulation of substrate and nutrition at a substratum,
2) Transfer of planktonic microbial cells from the bulk fluid to the substratum,
3) Reversible adsorption of the cells to the substratum,
4) Desorption of a portion of adsorbed cells and returning to the bulk liquid phase,
5) Irreversible adsorption of bacterial cells at the surface,
6) Transport of substrate to and within the biofilm,
7) Substrate metabolism by biofilm-bound cells accompanied by cellular growth and EPS production,
8) Detachment of a portion of the biofilm and also some daughter cells.

Biofilms can be developed aerobically or anaerobically. In developed biofilms, some parts may be aerobic and others anaerobic. Aerobic bacteria near the outer surface of a biofilm consume oxygen. If biofilm is thick enough, oxygen will be depleted at the base film creating an anaerobic zone (Borenstein, 1994).

The increase of biofilm thickness during growth usually follows a sigmoidal curve (Ross et al., 1998). It means that the biofilm will eventually reach a steady state beyond which the biofilm will maintain a relatively uniform thickness. At this thickness little substrate is available to the embedded bacteria in the base film, and the rates of attachment and removal from the surface film are basically in equilibrium.

Starvation and presence of toxic substances may lead to death or lysis of the cells in the biofilm. However, cell death or lysis in a well-developed biofilm does not necessarily mean the termination of biofilm structure, as the EPS structure can maintain the biofilm function to influence the mass transfer (Castegnier et al., 2006).

2.1.5 Mass transport in biofilms

Mass transport within biofilms is a complex phenomenon which is influenced by biofilm heterogeneity, discrete cell clusters and interstitial voids distribution, as well as the hydrodynamic regime of flow. de Beer et al. (1994) assumed that mass transport through the biofilm boundary layer and within the biofilm are governed by diffusion, hence perpendicular to the substratum. However, Siegrist and Gujer (1985) found that the effective diffusion coefficient in biofilms is dependent on the flow conditions and biofilm roughness, indicating convection through pores in the biofilm. Interstitial voids might

enhance substrate and product fluxes throughout the biofilm by decreasing tortuous pathways or by facilitating convection. This implies that the substrate concentration in voids is higher than that in adjacent biomass.

Diffusion of a solute through biofilm has been attributed to the solute physical chemistry and the biofilm density. Stewart (1998) conducted a statistical analysis on the available data collected from a number of studies on diffusion through biofilms. Ionic solutes (inorganic anions or cations) in his review have shown the highest diffusion rate, expressed as effective diffusive permeability; whereas, high molecular weight organic solutes have demonstrated the lowest diffusion rate. He also suggested that solute diffusion decreased sharply with increasing biomass volume fraction of a biofilm.

More recent experimental data indicate that the convective flow within the biofilm may be considerable (Stoodley et al., 1994; Lewandowski et al., 1995). Water which flows through the biofilm, creates two flow fields above and within the biofilm which interact with each other in a manner analogous to hydrodynamics above a porous bed. Hence, the assumption that indicates the mass transport within a biofilm is predominantly governed by molecular diffusion is not valid any more.

Lastly, transport phenomena in biofilms have been studied by various methods including microelectrodes, fiberoptic microsensors, nuclear magnetic resonance spectroscopy, infrared spectroscopy combined with Raman microscopy, fluorescence recovery after photobleaching, fluorescence correlation spectroscopy (FCS), and confocal laser scanning microscopy (CLSM). Indirect methods are usually preferred for measuring mass transport

in biofilms, since direct invasive procedures can potentially disturb their structural integrity (Thurnheer et al., 2003).

2.1.6 Biofilms in porous and fractured media

Bacteria preferentially attach to particles and solid surfaces in subsurface environments. These attached bacteria play a crucial role in biodegradation of contaminants and clogging of porous media, particularly when the biofilm growth is stimulated by groundwater flow and nutrition loading (Rittmann, 1993). Several studies have emphasized the role of biofilms in reducing the permeability of porous and fractured media by as much as three orders of magnitude, as well as altering the pore velocity distribution (e.g. Taylor and Jaffé, 1990; Ross and Bickerton, 2002). Industrial applications also include microbially enhanced leaching of metals from ore and recovery of metals from solutions, deliberate plugging of high-permeability zones to enhance oil recovery operations, and bioreactors for water and wastewater treatment (Cunningham et al., 1991). Particles of organic and inorganic material flowing in suspension may also be removed by the attached biomass via diffusion, interception, and sedimentation (Bouwer, 1987).

Biofilm morphology in porous media systems can be highly variable, ranging from patchy discontinuous colonies to thick continuous films. Consequently, different mechanisms by which biofilms reduce the permeability of porous media have been reported. In case of continuous films, pore spaces are reduced, causing both porosity and permeability to decrease (Cunningham et al., 1991). On the other hand, when patchy colonies are formed, permeability is reduced by biofilm aggregates accumulating mainly in pore throats. Under

this condition, a relatively small amount of biomass can cause a large reduction in permeability by increasing the flow path length.

Individual biofilm processes are considerably difficult to examine in porous media. Biofilm growth, for example, is complicated by the nature of fluid and nutrient transport which, in porous media, occurs along tortuous flow paths of variable geometry. Similarly, the wide distribution of pore velocities introduces considerable variation in the processes of adsorption, desorption, attachment, and detachment (Bouwer et al., 2000). As a result, most investigations have focused on quantifying the effects of biofilms on characteristics of porous and fractured media rather than the behaviour of individual biofilm processes. Fractured media, nevertheless, have received little attention regarding the impacts of biofilms compared to porous media (Ross and Bickerton, 2002).

The idea of developing biofilm in porous and fractured media has been vastly implicated in remediation of contaminated groundwater aquifers. Often, the initial step for remediation of groundwater pollution is containment of the contaminant plume. A carbon source and nutrients can be injected into a porous or fractured aquifer to enhance microbial activities which end up with biofilm development (biostimulation). Specific types of bacteria may also be released into the aquifer before nutrition loading (bioaugmentation). These processes will create either a bioactive zone to degrade contaminants in the flowing groundwater or a biobarrier by plugging of the formation (Cunningham et al., 1997).

2.2 Diffusion

2.2.1 Flux equations

The mass flux of a solute in a porous media occurs under the combined effects of hydraulic and concentration gradients. The one-dimensional transport can be formulated as below (Shackelford, 1991):

$$J = n\left(v_s C - D_h \frac{\partial C}{\partial x}\right) \quad (1)$$

where J is the mass flux (M L^{-2} T^{-1}); n is the total porosity of the media; v_s is the average fluid velocity or seepage velocity (L T^{-1}); C is the mass concentration of the solute (M L^{-3}); x is the direction of the transport (L); and D_h is the hydrodynamic dispersion coefficient (L^2 T^{-1}). The hydrodynamic dispersion coefficient accounts for both mechanical and diffusive dispersion:

$$D_h = D_m + D_0\tau \quad (2)$$

where D_m is mechanical dispersion coefficient which is a function of the velocity, D_0 is free water diffusion coefficient of the solute and τ is the tortuosity factor (see section 2.2.2). In the absence of hydraulic gradient, which is a typical case for mass transport through a rock matrix and low permeability soils, equation 1 reduces to the following equation which is Fick's first law for one-dimensional diffusive transport in porous media:

$$J_D = -D_0 n\tau \frac{\partial C}{\partial x} \quad (3)$$

Rock matrix porosity, in particular, is made up of a transport or effective porosity, n_t, and a storage porosity, n_d (Ohlsson and Neretnieks, 1995):

$$n = n_t + n_d \tag{4}$$

The transport porosity accounts for the pores utilized in transporting the solute, while the storage porosity refers to the pores that have dead ends. The latter have little contribution in solute transport but can affect the capacity to hold the dissolved species. Therefore, equation 3 becomes the following:

$$J_D = -D_0 n_t \tau \frac{\partial C}{\partial x} \tag{5}$$

2.2.2 Tortuosity factor

The tortuosity factor, also referred to as the geometric factor, accounts for the increased length of the transport path of the solute due to the tortuous pathways experienced by the solute migrating through the porous medium. Researchers have suggested several methods to calculate this factor. Olsen and Kemper (1968) and Bear (1972) have expressed this factor as bellow:

$$\tau = \left(\frac{L_e}{L_t}\right)^2 \tag{7}$$

where L_e and L_t are the equivalent and total length of the solute transport through the porous media respectively. In this case, the value of τ is always less than 1, since the solute travels a distance further than the straight line path.

2.2.3 Effective diffusion coefficient

The effective diffusion coefficient (D^*) includes the effect of tortuosity. This factor is defined as there is currently no satisfactory method to determine tortuosity independently.

Conventional methods of measuring the porosity of porous media, whose structures have been biologically altered, may not be practical as well. D^*, therefore, is expressed as:

$$D^* = D_0 \tau \tag{8}$$

And the expression of Fick's first law for diffusion in porous media becomes:

$$J_D = -D^* n \frac{\partial C}{\partial x} \tag{9}$$

2.2.4 Fick's second law of diffusion

The transient transport of a solute through a porous medium is given by the continuity equation as presented bellow (Bear and Verruijt, 1987):

$$\frac{\partial C}{\partial t} = -\nabla J \pm R \pm \lambda C \tag{10}$$

where C is the solute concentration; ∇ is the divergence operator, λ is a rate constant [T^{-1}] used to describe the decay or build-up of chemical species; and R is a general term representing all other chemical and biological reactions [$M\ L^{-3}\ T^{-1}$]. The positive signs (+) in equation 10 are used for concentration source terms (e.g. mineral dissolution) whereas the negative signs (-) are used for terms representing concentration sinks (e.g. precipitation). In modeling contaminant transport, sorption may occur and is often assumed to be linear and reversible. Assuming a homogeneous media and incompressible fluid, equation 10 can be expressed as follows where no decay or outside reaction occurs (Freeze and Cherry, 1979):

$$\frac{\partial C}{\partial t} = \left(\frac{D^*}{R_d}\right)\frac{\partial^2 C}{\partial x^2} - \left(\frac{v_s}{R_d}\right)\frac{\partial C}{\partial x} \tag{11}$$

where R_d is the dimensionless retardation factor representing the relative rate of transport of a non-reactive solute to that of a reactive solute subject to reversible sorption (Freeze and Cherry, 1979). This factor is equal to 1 for non-sorbing solutes.

Following the same assumption as mentioned before, the fluid velocity in porous rock is considered as negligible; hence, diffusion becomes more significant relative to advection. Therefore, equation 11 reduces to the following expression for Fick's second law for diffusion of non-reactive solutes in porous media:

$$\frac{\partial C}{\partial t} = \frac{D^*}{R_d}\frac{\partial^2 C}{\partial x^2} \qquad (12)$$

2.2.5 Significance of diffusion in rock matrix

It is recognized that diffusion is the dominant transport mechanism within the rock matrix of a fractured rock medium. Gillham et al. (1984) indicated that diffusion is dominant when seepage velocity is in the order of 0.005 m yr^{-1}. This velocity corresponds to a saturated hydraulic conductivity of $8*10^{-11}$ m s^{-1} when the porosity is 0.5 and the hydraulic gradient is one. Considering the range of rock characteristics, it is evident that diffusion is the dominant process in contaminant transport in a rock matrix. Therefore, it is important to quantify the contaminant diffusion process into rock matrices.

Contaminated fractured rock environments have received increasing attention over the last two decades. It is because of the extent of the problem due to the contamination of fractured environments on one hand, and the complexity of such environments on the other hand, which can make the cleanup process extremely difficult and costly. Flow in fractured

rock is governed by the fracture pathways, the interconnection of the fracture network, and the interaction of the fracture and the rock matrix. The transfer of contaminants between a discrete fracture and the rock matrix, as well as the persistence of the contaminant in a fractured rock medium, is mostly governed by matrix diffusion. Therefore, in order to effectively resolve the process of contaminant transport in fractured rock environments, models that accurately describe the transport process must be developed.

Deep geologic burial as a long-term solution for the safe storage of nuclear waste is another case in which matrix diffusion has been considered (Neretnieks, 1980). The concept behind deep geologic burial is that both engineered materials and the geosphere can provide multiple barriers to the potential migration of radionuclides from the repository to points where they can come in contact with the biosphere (McKenna and Selroos, 2004). Performance assessment calculations are used to predict the potential release and migration of radionuclides through the geosphere for thousands of years into the future. Over these time scales, transport of radionuclides, occurring primarily through the fractures, can be slowed considerably by diffusion of the radionuclides into the rock matrix. Several matrix diffusion models have been developed to effectively describe such processes (e.g. Hölttä et al., 1996).

2.2.6 Diffusion models

Diffusion has been extensively investigated in laboratories for a wide range of applications. Among these applications, contaminant transport through landfill liners (Rowe et al., 1987), nuclear waste disposal (Ohlsson and Neretnieks, 1995), and bacterial transport in subsurface environments (Harvey et al., 1989) have been paid remarkable attention.

In general, methods used in diffusion modeling and experiments are classified into two broad categories, steady state and transient, corresponding to the type of transport equation used in the analytical determination of the D* values (Shackelford, 1991). Basically, steady-state methods apply Fick's first law (equation 9) to measure the effective diffusion coefficient. Whereas, transient methods utilize solutions either to equation 11 when advective flow is allowed to occur or to Fick's second law (equation 12) in the absence of advective flow. Detailed reviews of the state-of-the-art in diffusion models and experiments are available in the literature (e.g. Shackelford, 1991; Ohlsson and Neretnieks, 1995).

2.2.6.1 Double reservoir method

Double reservoir method was used to examine the diffusion process in this thesis. The model, described by Rowe et al. (1988), is categorized among the transient methods and is depicted in Fig. 2.1 (a). The cell consists of two reservoirs: the source reservoir which has an initial concentration of the solute, and an exit reservoir in which the solute concentration is zero at the beginning of the test. The porous material of interest is placed between two reservoirs. As the test begins, the concentrations of the tracer (solute) decreases with time in the source reservoir and eventually increases with time in the exit reservoir. The concentration profiles in the source reservoir, porous sample and exit reservoir as a function of time are illustrated in Fig. 2.1 (b) (Shackelford, 1991). A semi-analytical solution to the Fick's second law (equation 12) is used to fit the theoretical curves to the measured data to determine D* values. As can be observed in Fig. 2.1 (b), concentration profile can approach a state such that the concentration profile within the porous medium is close to linear (e.g. at t_3). Once this condition is reached, D* can be determined as follows:

$$D^* = -\left(\frac{\Delta x}{n\Delta C}\right)J_D = -\left(\frac{L_P}{n\Delta C}\right)\left(\frac{\Delta m}{A\Delta t}\right) = -\left(\frac{L_P}{nA\Delta C}\right)\left(\frac{\Delta m}{\Delta t}\right) \quad (15)$$

where L_P and A are the length and cross-sectional area of the porous media, respectively; ΔC is the concentration gradient; and Δm is the change in mass of the tracer in an increment of time, Δt.

2.3 References

Allison, D.G., Sutherland, I.W. 1987. The role of exopolysaccharides in adhesion of freshwater bacteria. Microbiology 133(5): 1319-1327.

Bear, J. 1972. Dynamics of Fluids in Porous Media. American Elsevier, New York, NY.

Bear, J., Verruijt, A. 1987. Modeling groundwater flow and pollution. D. Reidel Publishing Company, Boston Massachusetts.

Bishop, P.L. 1997. Biofilm structure and kinetics. Water Science and Technology 36: 287-294.

Bishop, P.L., Rittmann, B.E. 1995. Modelling heterogeneity in biofilms: report of the discussion session. Water Science and Technology 32: 263-265.

Borenstein, S.W. 1994. Microbiologically influenced corrosion handbook. Woodhead, Cambridge, England.

Bouwer, E. J. 1987. Theoretical investigation of particle deposition in biofilm systems. Water Research 21: 1489-1498.

Bouwer, E.J., Rijnaarts, H.H.M., Cunningham, A.B., Gerlach, R. 2000. Biofilms in porous media. In: Biofilms II: Process analysis and applications, (Ed) Bryers, J.D. John Wiley & Sons Inc. 123-158.

Boyd, A., Chakrabarty, A.M. 1994. Role of alginate lyase in cell detachment of Pseudomonas aeruginosa. Applied Environmental Microbiology 60: 2355-2359.

Bryers, J.D. 2000. Biofilm formation and persistence. In: Biofilms II: Process analysis and applications, (ed) Bryers, J.D. John Wiley & Sons Inc. 45-88.

Caldwell, D.E., Korber, D.R., Lawrence, J.R. 1992. Imaging of bacterial cells by fluorescence exclusion using scanning confocal laser microcopy. Journal of Microbiological Methods 15: 249-263.

Castegnier, F., Ross, N., Chapuis, R.P., Deschênes, L., Samson, R. 2006. Long-term persistence of a nutrient-starved biofilm in a limestone fracture. Water Research 40: 925-934.

Characklis, W.G., Wilderer, P.A. 1989. Introduction. In: Structure and function of biofilms. Eds. Characklis, W.G., Wilderer, P.A. John Wiley & Sons Inc., Toronto pp. 1-4.

Charaklis, W., Marshall, K. 1990. Biofilms. John Wiley & Sons, Inc., New York, NY.

Charaklis, W.G., Marshall, K.G. 1990. Biofilms: A basis for interdisciplinary approach. In: Biofilms, eds. Characklis, W.G., Marshall, K.G. John Wiley & Sons Inc., Toronto, 3-16.

Christensen, B.E., Characklis, W.G. 1990. Physical and chemical properties of biofilms. In: Characklis W.G., Marshall, K.G. (Eds.) Biofilms, John Wiley and Sons, New York, NY, pp. 93-130.

Cooke, A.J., Rowe, R.K., Rittmann, B.E., Fleming, I.R. 1999. Modelling biochemically driven mineral precipitation in anaerobic biofilms. Water Science and Technology 39(7): 57-64.

Costerton, J.W., Lewandowski, Z., Caldwell, D.E., Korber, D.R., Lappin-Scott, H.M. 1995. Microbiol biofilms. Annual Review of Microbiology 49: 711-745.

Cunningham, A.B. 1989. Hydrodynamics and solute transport at the fluid-biofilm interface. In: Structure and function of biofilms. Eds. Characklis, W.G., Wilderer, P.A. John Wiley & Sons Inc., Toronto, 19-32.

Cunningham, A.B., Characklis, W.G., Abedeen, F., Crawford, D. 1991. Influence of biofilm accumulation on porous media hydrodynamics. Environmental Science and Technology 25: 1305-1311.

Cunningham, A.B., Warwood, B., Sturman, P., Horrigan, K., James, G., Costerton, J.W., Hiebert, R. 1997. Biofilm processes in porous media-Practical applications. In: The microbiology of the terrestrial deep subsurface. (Eds) Amy, P.S., Haldeman, D.L. Lewis Publishers, Boca Raton, FL, 325-344.

deBeer, D., Stoodley, P., Roe, F., Lewandowski, Z. 1994. Effects of biofilm structures on oxygen distribution and mass transport. Biotechnology and Bioengineering 43: 1131-1138.

Derjaguin, B.V., Landau, L. 1941. Acta Physicochimica (USSR) 14: 633

Freeze, R.A., Cherry, J.A. 1979. Groundwater. Prentice-Hall, Englewood Cliffs, New Jersey, 604pp.

Frølund, B., Palmgren, R., Keiding, K., Nielsen, P.H. 1996. Extraction of extracellular polymers from activated sludge using a cation exchange resin. Water Research 30(8): 1749-1758.

Gilbert, P., Das, J., Foley, I. 1997. Biofilm susceptibility to antimicrobials. Advances in Dental Research 11(l):160-167.

Gillham, R.W., Robin, M.L.J., Dytynyshyn, D.J., Johnston, H.M. 1984. Diffusion of non-reactive and reactive solutes through fine-grained barrier materials. Canadian Geotechnical Journal 21: 541-550.

Grimm, L.H., Kelly, S., Volkerding, I.I., Krull, R., Hempel, D.C. 2005. Influence of mechanical stress and surface interaction on the aggregation of Aspergillus niger conidia. Biotechnology and Bioengineering 92(7): 879-88.

Harvey, R.W., George, L.H., Smith, R.L., LeBlanc, D.R. 1989. Transport of microspheres and indigenous bacteria through a sandy aquifer: Results of natural and forced-gradient tracer experiments. Environmental Science and Technology 23: 51-56.

Hölttä, P., Hakanen, M., Hautojärvi, A., Timonen, J., Väätäinen, K. 1996. The effects of matrix diffusion on radionuclide migration in rock column experiments. Journal of Contaminant Hydrology 21(1-4):165-173.

Jahn, A., Nielsen, P.H. 1995. Extraction of extracellular polymeric substances from biofilms using a cation exchange resin Water Science and Technology 32(8): 157-164.

Lawrence, J.R., Korber, D.R., Hoyle, B.D., Costerton, J.W., Caldwell, D.E. 1991. Optical sectioning of microbial biofilms. Journal of Bacteriology 173: 6558-6567.

Leon Ohl, A., Horn, H., Hempel, D.C. 2004. Behaviour of biofilm systems under varying hydrodynamic conditions. Water Science and Technology 49(11-12): 345-51.

Lewandowski, Z., Stoodley, P., Altobelli, S. 1995. Experimental and conceptual studies on mass transport in biofilms. Water Science and Technology 31: 153-162.

Marshall, K.C. 1992. Biofilms: an overview of bacterial adhesion, activity, and control at surfaces. ASM News 58(4): 202-207.

Marshall, K.G. (Ed).1984. Microbial adhesion and aggregation. Berlin, Germany, Springer-Verlag.

McKenna, S.A., Selroos, J.O. 2004. Constraining performance assessment models with tracer test results: a comparison between two conceptual models. Hydrogeology Journal 12: 243-256.

Neretnieks, I. 1980. Diffusion in the rock matrix, an important factor in radionuclide migration. Journal of Geophysical Research 85(B8): 4379-4397.

Nielsen, P.H., Jahn, A., Palmgren, R. 1997. Conceptual model for production and composition of exopolymers in biofilms. Water Science and Technology 36(1): 11-19.

Ohlsson, Y., Neretnieks, I. 1995. Literature survey of matrix diffusion theory and of experiments and data including natural analogues. SKB TR-95-12, Svensk Kärnbränslehantering AB.

Olsen, S.R., Kemper, W.D. 1968. Movement of nutrients to plant roots. Advanced Agronomy 20: 91-151.

O'Toole, G. 2003. To build a biofilm. Journal of Bacteriology 185: 2687-2689.

Rittman, B. E. 1993. The Significance of Biofilms in Porous Media. Water Resources Research. 29: 2195-2202.

Ross, N., Bickerton, G. 2002. Application of biobarriers for groundwater containment at fractured bedrock sites. Remediation 12 (3): 5-21.

Ross, N., Deschenes, L., Bureau, J., Clément, B., Comeau Y., Samson, R. 1998. Ecotoxicological assessment and effects of physicochemical factors on biofilm development in groundwater conditions. Environmental Science and Technology 32(8): 1105-1111.

Rowe, R.K. 1987. Pollutant transport through barriers. In: Geotechnical Practice for Waste Disposal (Ed) Woods, R.D. ASCE special publication 13: 159-181.

Rowe, R.K., Caers, C.J., Barone, F. 1988. Laboratory determination of diffusion and distribution coefficients of contaminants using undisturbed clayey soils. Canadian Geotechnical Journal 25: 108-118.

Schafer, A., Ustohal, P., Harms, H., Stauffer, F., Dracos, T., Zehnder, A.J.B. 1998. Transport of bacteria in unsaturated porous media. Journal of Contaminant Hydrology 33: 149-169.

Shackelford, C.D. 1991. Laboratory diffusion testing for waste disposal. A review. Journal of Contaminant Hydrology. 7(3) 177-217.

Siegrist, H., Gujer, W. 1985. Mass transfer mechanisms in a heterotrophic biofilm. Water Research 19(11): 1369-1378.

Stewart, P.S. 1998. A review of experimental measurements of effective diffusive permeabilities and effective diffusion coefficients in biofilms. Biotechnology and Bioengineering 59(3): 261-272.

Stoodley, P., de Beer, D., Lewandowski, Z. 1994. Liquid flow in biofilm systems. Applied and Environmental Microbiology 60: 2711-2716.

Taylor, S.W., Jaffé, P.R. 1990. Biofilm growth and the related changes in the physical properties of a porous medium, 1. Experimental investigation. Water Resources Research 26(9): 2153-2159.

Thurnheer, T., Gmür, R., Shapiro, S., Guggenheim, B. 2003. Mass Transport of macromolecules within an in vitro model of supragingival plaque. Applied and Environmental Microbiology 69(3): 1702-1709.

Verwey, E.J., Overbeek, J.T.G. 1948. Theory of the Stability of Lyophobic Colloids. Elsevier, Amsterdam.

Zhang, T., Bishop, P.L. 1994. Density, porosity, and pore structure of biofilms. Water research 28(11): 2267-2277.

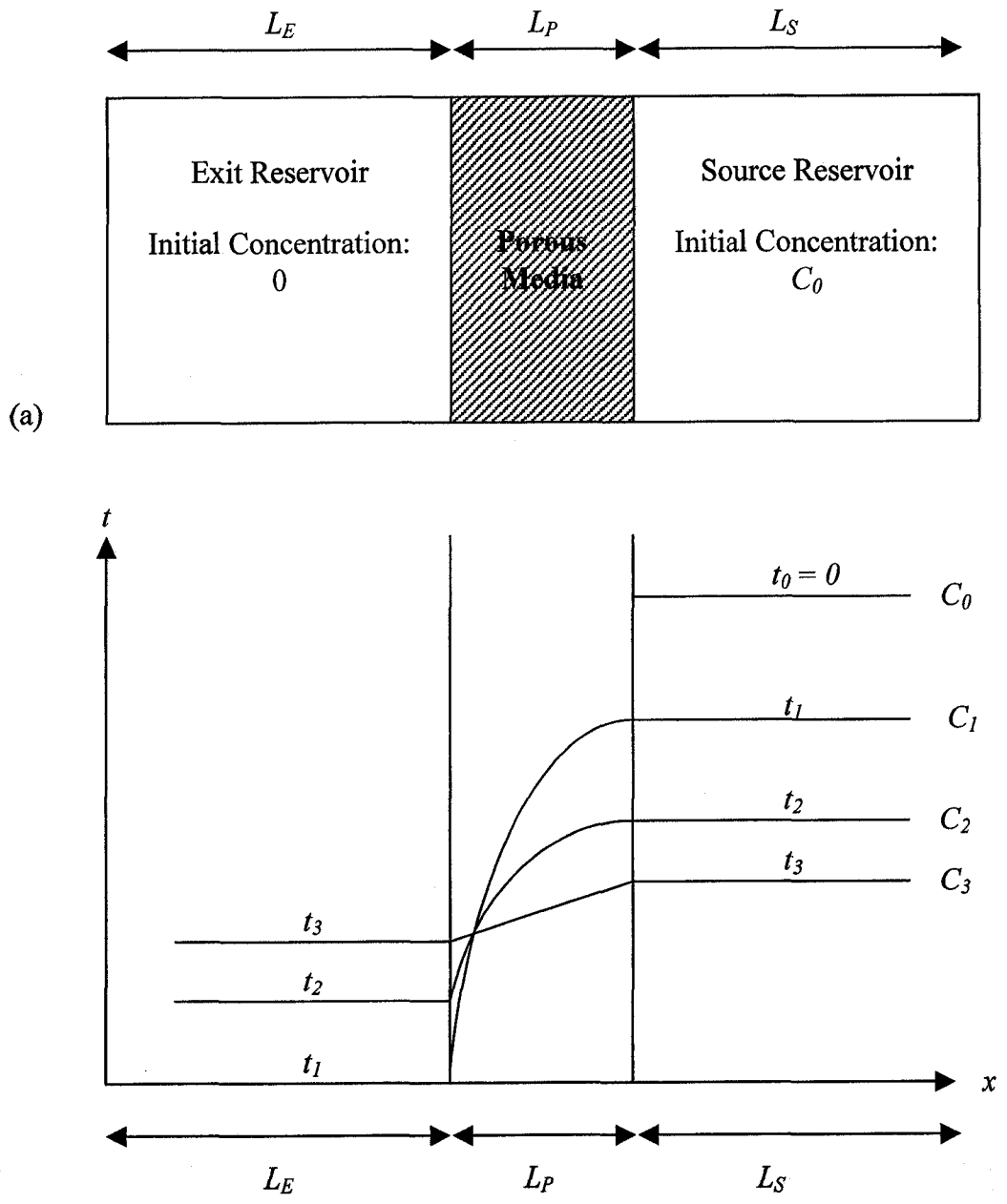

Figure 2.1: (a) Schematic diagram of double reservoir method. (b) Concentration profiles (Modified form Shackelford (1991)).

Chapter 3:

Impacts of Biofilm on Diffusion in Fractured Rock

By

Hooman Ghassemi[1], Nathalie Ross[1],

Paul Van Geel[2]

[1]Dept. of Chemical Engineering, University of Ottawa

161 Louis Pasteur, Room A412

Ottawa, Ontario

K1N 6N5

[2]Dept. of Civil Engineering, Carleton University

1125 Colonel By Drive

Ottawa, Ontario

K1S 5B6

Submitted to

Journal of Contaminant Hydrology

3 IMPACTS OF BIOFILMS ON DIFFUSION IN FRACTURED ROCK

Abstract

Fractured rock aquifers have complex flow systems and this complexity imposes several constraints on cleanup efforts. Remedial techniques in such aquifers are influenced by diffusion of contaminants into the rock matrix and the subsequent back diffusion into fractures. In particular, the back diffusion process can release a low concentration of contaminant into the groundwater for an extended period of time after the main source of contamination is removed by hydraulic forces. Stimulated biofilms can be potentially exploited as biological barriers to reduce the rate of contaminant diffusion between a porous matrix and adjacent fracture. The main objective of this study was to assess the potential of a biofilm to limit diffusion between the host rock and fracture. The impacts of different types of microorganism on diffusion rate were also compared and the performances of the tracers employed in diffusion experiments were evaluated.

Three species of microorganisms, which excrete different amount of EPS, were exploited to develop a biofilm: *Pseudomonas putida*, *Escherichia coli* (K12) and an indigenous groundwater population. Biofilms were grown on high porosity ceramic disks which were subsequently installed in stainless steel double-reservoir diffusion cells. Source reservoirs were spiked with known concentrations of bromide and Lissamine. The concentration decline in the source reservoirs and the flux into the exit reservoirs were monitored versus time for bromide and Lissamine using a bromide selective ion electrode and a fluorometer

respectively. A conceptual model was used to assist in the interpretation of the experimental data obtained from a total of 17 diffusion experiments.

A comparison of the estimated effective diffusion coefficients from biofilm stimulated disks and control disks did not suggest a significant impact of the biofilm on matrix diffusion. However, this lack of significant impact of biofilm could possibly be due to the lack of sufficient biofilm growth within the pores, biofilm decay/detachment during the test period, the heterogeneity of biofilm structures, or highly porous structures of developed biofilms. Finally, unlike bromide, Lissamine did not appear to behave as a conservative tracer indicating potential decay and/or adsorption.

3.1 Introduction

Fractured rock aquifers are often considered as complex environments for cleanup processes. The groundwater flow in such environments is governed by the fracture pathways and the interconnection of the fracture network. In the absence of advective flow in low permeability rock matrices, the transfer of contaminant between the fracture and rock matrix is due to the concentration gradient and is governed by diffusion. The contaminated rock matrix is also considered as a persistent source of contamination by releasing small amounts of contaminant via diffusion to the groundwater flow for extended periods of time after the original source of contamination is removed by hydrodynamic forces (Mutch et al., 1993). The success of remedial techniques in these sites basically depends on the level of understanding of the transport mechanisms.

Biofilms have been defined as cells immobilized on a solid surface and embedded in a gel matrix of polymeric material excreted by microorganisms. Two main components of biofilms in groundwater systems are the microbial community (groundwater indigenous bacteria) and the extra-cellular polymeric substances (EPS) (Ross and Bickerton, 2002). From a macroscopic point of view, a biofilm formed on a fracture surface is assumed to act as a fracture skin. On the other hand, recent studies have revealed evidences that bacteria penetrate into the pore matrix of the rock and form a biofilm on pore surfaces (Charbonneau et al., 2006). As a result, biofilm can perform as a barrier in groundwater systems, which influences hydraulic properties of the fractured media and may impact the rate of contaminant transport between the rock matrix and the fracture. It may also reduce the contaminant source mobility by decreasing the effective diffusion of pollution from a contaminated rock matrix into the fracture. In-situ and laboratory studies have been conducted to demonstrate the potential of the biofilm to reduce the permeability of a fracture (Ross et al., 1998; Ross et al., 2001; Ross and Bickerton, 2002). In addition, the modeling of the effects of biofilm on transport in such environments has been reported (Hill and Sleep, 2002). More recent laboratory studies (Charbonneau et al., 2006) have evaluated the impact of a biofilm on the diffusion of a contaminant from a rock matrix to an adjacent water reservoir.

EPS is a porous matrix composed of a combination of polymeric materials, including lipids, proteins, polysaccharides, polyphenols, nucleic acids and humic materials. A number of studies have shown the influence of nutrient loading and flow condition on EPS composition and structure (Jennings et al., 1995; Stoodley et al., 1999; Ross et al., 1998). The voids in the EPS porous matrix are usually filled with water and soluble species which

move freely through the system, primarily, by molecular diffusion (Characklis and Wilderer, 1989). Mass transport within biofilms is influenced by biofilm heterogeneity, discrete cell clusters and interstitial voids distribution, as well as the hydrodynamic regime of flow. It is assumed to be mainly governed by diffusion (de Beer et al., 1994), while interstitial voids might enhance substrate and product fluxes throughout the biofilm by reducing the tortuous path or by facilitating the advective flow (Siegrist and Gujer, 1985, Stoodley et al., 1994). In general, mass transport in biofilms can be governed by two mechanisms dominant in two zones: convective external mass transfer (from the bulk solution to the biofilm) and diffusive internal mass transport (within the biofilm). The rate of nutrient transport to the biofilm is quantified by linking the convective mass transfer rate to the diffusive mass transport rate across the biofilm surface (Beyenal and Lewandowski, 2002).

Existence of EPS producing bacteria in groundwater is crucial in developing biofilms in fractured rock aquifers. In addition, bacteria size, surface characteristics, and motility are imperative concerns in their transport to the target zones. Bacteria have been found to persist to a significant depth in fractured rock environments (Pedersen, 1993; Pedersen, 2000). A significant fraction of the EPS producing bacteria in groundwater are ultramicrobacteria (UMB) which are defined as bacteria having a diameter smaller than 0.3 μm (Ross et al., 2001b). The UMB can exist as either naturally occurring small active bacteria or normal size bacteria reduced in volume after experiencing a starvation-survival condition (Kemp et al., 1993). Their low surface hydrophobicity and small size improve their transport ability and allow them to reach small pores and fractures, hence making them of particular interest in forming biobarriers in fractured rock environments.

The thickness of biofilm is influenced by the balance between biofilm detachment and growth rates. The increase of biofilm thickness typically follows a sigmoidal curve (Ross et al., 1998). Biofilm physiological characteristics, including thickness, density, shear resistance and diffusivity, are influenced by substrate flux and hydrodynamic forces applied during the growth phase. It is well known that biofilms grown at higher flow velocities are denser than those grown at lower flow velocities (Gantzer et al., 1991; Characklis and Marshall, 1990). By changing the hydrodynamic conditions and maintaining a constant rate of substrate loading, Leon Ohl et al. (2004) found that increasing the flow velocity in the bulk phase led both to a higher biofilm density and a higher substrate flux. Besides, the biofilm surface became more homogenous and the thickness of the boundary layer decreased. This increase in biofilm density is assumed to be a physiological response to the imposed shear stress, which leads to rearranging of the internal biofilm structure (Beyenal and Lewandowski, 2002). However, rearranging the internal structure may affect the biofilm diffusivity and internal mass transport rates as a result of increasing biofilm density (Fan et al., 1990).

Mass transport in layered formations has been investigated by a number of researchers. Novakowski (1989) developed an analytical model to simulate the role of a well-bore skin of finite thickness on well productivity and behaviour. Rowe et al. (1997) described a semi-analytical model for solute transport through a series of finite homogeneous layers. Robinson et al. (1998) presented solutions for solute transport in a finite system of parallel fractures with fracture skins. Fracture skins have been defined as zones of altered rock abutting the fracture and the coatings of the fracture surfaces by infiltered debris,

precipitated minerals and organic matters (Robinson et al., 1998). Fracture skin can alter the transport properties of the media.

Biofilm developed on a rock surface may impact the transport process between the fracture and the rock matrix (Lawrence et al., 1995; Charbonneau et al., 2006). A biofilm coating a rock surface may invade the rock micropores to a definite depth or act as a skin. It is hypothesized that the biofilm can reduce the effective diffusion coefficient (D^*) of a porous matrix by altering the tortuous path that the contaminant molecules pass through. The objectives of this study were to assess the potential of biofilm to limit the effective diffusion coefficient of a porous matrix and to compare the performances of different microorganisms used to develop biofilm.

To conduct this study, a set of double reservoir diffusion cells were constructed. Different types of biofilm were grown on one side of ceramic disks which were subsequently installed into the cells. Source reservoirs in the cells were spiked with two types of tracer (bromide and Lissamine) and diffusion experiments were carried out. A semi-analytical model was used to assist in the interpretation of the experimental results. Lastly, the performance of Lissamine as a conservative tracer was evaluated.

3.2 Experimental method

3.2.1 Microorganisms

Three species of microorganisms were exploited to develop a biofilm: *Pseudomonas putida*, *Escherichia coli* (K12) and an indigenous groundwater population. *Pseudomonas*

putida is a gram-negative rod-shaped bacterium able to grow on a wide variety of substrate. These bacteria play an important role in decomposition, biodegradation, and carbon and nitrogen cycles. Consequently, they are important organisms in bioremediation of organic solvents including toluene. *P. putida* is known to excrete significant amounts of EPS to develop a uniform EPS matrix resulting in a well-defined biofilm (Ude et al., 2006). *Escherichia coli* (K12), on the other hand, produces comparatively little EPS (Razatos et al., 1998). Therefore, a non-uniform patchy biofilm is expected to grow.

Unfiltered groundwater from a sedimentary rock aquifer in Kingston, Ontario was pumped to be used in this study. Water was collected in plastic potable water containers, transferred to the laboratory and stored at 4°C. The pumped water was tested for the presence of several types of bacteria common to groundwater including iron-reducing bacteria, slime-forming bacteria, and sulphate reducing bacteria. Slime producing bacteria were found in the groundwater samples suggesting the potential for biofilm formation (Yungwirth, 2006).

3.2.2 Tracers

Two types of tracer were used in the diffusion experiments: bromide (Br^-) and Lissamine Flavine FF (Lissamine). Bromide is a common groundwater ionic tracer because of its stability, conservative behaviour, and low background concentrations in groundwater (Davis et al., 1985). A combination bromide electrode (Orion 9635, Thermo Electron Corporation, MA, USA) (Fig. 3.1) was used to detect the bromide concentration. Lissamine is a fluorescent dye used in groundwater tracer tests (Novakowski and Lapcevic, 1994; van der Kamp et al., 1996). It has been reported to behave conservatively in field experiments although it is susceptible to photo degradation (Smart and Laidlaw, 1977) and some

adsorption under field conditions has been reported (Novakowski, 1992). Most of the previous studies on this tracer have been conducted in sterile conditions; hence, biodegradation could be a cause of dye loss in the presence of large microbial populations although no loss due to biodegradation has been reported. A fluorometer (Modulus, Turner BioSystems Inc., CA, USA) was used to measure the Lissamine concentration (Fig. 3.2).

3.2.3 Porous media

High porosity ceramic disks, purchased from Soilmoisture Equipment Corp. (Santa Barbara, CA, USA), were used as the porous medium in this study (Fig. 3.3) (part number: 0606D03-B0.5M2). The disks are 79.38 mm in diameter and 7.14 mm in thickness. They have an air entry value of 0.5 bar, their porosity is greater than 60%, and their nominal pore size is 6.0 μm. A scanned electron Microscopy (SEM) image of the ceramic disk is provided in Figure 3.4. The ceramic formulation mainly consists of alumina (over 90% of Al_2O_3) plus small amount of Fe_2O_3, CaO, TiO_2, K_2O, and Na_2O.

3.2.4 Diffusion cell

Double-reservoir diffusion cells constructed of stainless steel were used for this study (Fig. 3.5). A schematic diagram of the designed cell is depicted in Figure 3.6. Each reservoir has a septum for taking samples, as well as a capped tube which provides access into the reservoir for the bromide electrode. Cells are air and water tight by installing two O-rings on both sides of the ceramic disk which is placed between the reservoirs. The reservoirs' volume was approximately 600 ml, while the source reservoir volume could be reduced by using an inert filler material.

3.2.5 Biofilm growth

The growth phase was entirely carried out in sterile conditions. Bacterial cultures, maintained in the freezer (-18° C) were introduced on agar plates, which were subsequently placed in an incubator for 24 hours until the colonies appeared. 1.5 litre beakers were foam plugged and wrapped with aluminium foil and autoclaved for 20 minutes at 121° C. Ceramic disks were thoroughly rinsed with ethanol and left in a sterile chamber to dry, then wrapped by Parafilm and aluminium foil on one side to prevent biofilm growth. A 30 g/l solution of Tryptic Soy Broth (TSB) in water was prepared as growth medium and autoclaved for 20 minutes at 121° C. The beakers containing approximately 400 ml of the media were left at room temperature. The disks were placed into the beakers and at least three colonies of bacterial culture were introduced to the media. The beakers were foam plugged and wrapped by aluminium foil to minimize the risk of contamination (Fig. 3.7). Afterward, the containers were placed on a rotating table for 72 hours at 24° C rotating at a speed of 45 rpm (Fig. 3.8). Fresh media were added after 72 hours to maintain a sufficient level of nutrients, and then the growth phase was extended for another 72 hours. Visual examination of the disks showed a whitish slime accumulation on the surface of the ceramics for all three types of microorganisms. This suggested the development of a biofilm. The wrap was removed from the other side of the disk prior to installation in the diffusion cell, which had already been autoclaved for 20 minutes at 121° C.

3.2.6 Diffusion experiments

Diffusion was established across the ceramic disk by spiking the source reservoirs to concentrations of 1500 ppm for bromide and 5000 ppb for Lissamine. A minimal salt

solution was used to fill both source and exit reservoir, while only the solution placed in the source reservoir solution was spiked with tracers. The solution had the minimum concentration of salts that are usually available in groundwater and are required for microorganisms to grow. The minimal salt solution recipe is described in Appendix A. No carbon source was provided for the microorganisms during the diffusion experiments; however, biofilms were reported to maintain their integrity under starvation conditions for extended periods of time (Castegnier et al., 2006).

Diffusion experiments were conducted by monitoring the tracers' concentration in the source and exit reservoirs. Tests were performed for up to 600 hours during which samples were taken from both source and exit reservoirs. To establish complete mixing conditions in both reservoirs, a magnetic bar was put in each reservoir and the cell was placed on a magnetic stirrer before sampling. The experiments were carried out at room temperature, since it was important to keep the temperature at a constant level to maintain a constant aqueous diffusion rate for the tracers (Shackelford, 1991).

In total, seventeen diffusion experiments were performed. At first, eleven cells were employed including: two cells as controls (no biofilm), three cells with *E. coli* biofilm, three cells with *P. putida* biofilm, and three cells with biofilm developed by an indigenous groundwater population. Afterward, six diffusion experiments were repeated utilizing: two cells as controls, two cells with *E. coli* biofilm, and two cells with *P. putida* biofilm. For the second set of experiments with six cells, the source reservoir volumes were reduced to approximately 180 ml using an inert filler material in order to accelerate the decline in concentration in the source reservoirs (Fig 3.9). The filler was composed of PVC and it was

expected neither to provide any carbon source for the microorganisms in the time scale of the experiment, nor to impact the tracer concentration by adsorption. An experiment was conducted by putting up to twenty chunks of the filler material (approximately 50 ml total volume) in a sealed cell containing a solution of 500 ppm of Br^- and 2000 ppb of Lissamine, then monitoring the solution's Br^- and Lissamine concentration for 25 days. No concentration loss was observed during that period.

3.2.7 Sampling and analysis

Bromide concentration was measured directly by putting the bromide electrode into the reservoir. The electrode was calibrated each time it was used using standard solutions of known Br^- concentration. The standard solutions were prepared using minimal salt solution in order to account for any potential interference from other ions present in the solution, although no interference was observed. The electrode was rinsed with ethanol then left to dry before inserting it into the reservoir to keep the cell sterile during the test.

200 µl samples were drawn from the reservoirs and placed into 200 µl micro cuvettes to be analyzed in the fluorometer for Lissamine concentration. A pipette fitted with a sterile tip was used to extract samples. Since the fluorescent measurement was non-destructive, the samples were returned into the reservoirs using a sterile syringe after being analyzed. The fluorometer was calibrated using standard solutions of Lissamine prepared with minimal salt solution.

3.2.8 Porosity measurement

When the tests were completed, the diffusion cells were dissembled and volumetric porosity of the ceramic disks were measured. The volumes of the disks were determined by measuring their diameter and thickness using a Vernier scale. Disks were then weighed and placed in an oven at 105° C for 24 hours before being reweighed. The amount of water lost upon drying was converted to a volume giving the total porosity as the ratio of the volume of water lost to the volume of the disk.

3.3 Mathematical modeling

In order to interpret the transport properties of the porous zone from the experimental data, it was necessary to use a suitable model. The objective of the model used for this study was to simulate the diffusion process which occurs in the double-reservoir diffusion apparatus. The model describes the transport of the solute through a porous medium. A semi-analytical solution is presented which applies the Laplace transform to solve the governing equations. A numerical approach is used for inverting Laplace variables into the real domain.

The model simulates the diffusion of a tracer through the saturated porous medium from the source reservoir toward the exit reservoir. It is assumed that completely mixed conditions are established in both reservoirs. Moreover, there is no advective flow through the porous zone. It is also assumed that the porous media is homogenous.

The governing equation for uniform diffusion of a solute in a porous medium is presented as follows (Crank, 1975):

$$\frac{\partial C}{\partial t} = \frac{D^*}{R}\frac{\partial^2 C}{\partial x^2} - \lambda C \qquad (1)$$

where C is the solute concentration, D^* is the effective diffusion coefficient accounting for molecular diffusion in aqueous phase as well as the effect of pore geometry ($D^* = D_0\tau$), R is the retardation factor, λ is the decay constant (accounting for all types of mass decay from the system), x is distance, τ is tortuosity factor, and t is time. Note that for the purpose of this thesis, λ is assumed to be equal to zero, since it was assumed that there was no biological or chemical reaction which causes the decay of the tracers. In addition, the value of R is equal to one because of the conservative nature of the tracers used in diffusion experiments. Consequently, equation (1) can be simplified as:

$$\frac{\partial C}{\partial t} = D^*\frac{\partial^2 C}{\partial x^2} \qquad (2)$$

Considering mass balance, equations of states for both source and exit reservoirs can be written as follows (Van Rees et al. (1991) :

$$V_s\frac{\partial C_s}{\partial t} = \gamma D^*\frac{\partial C}{\partial x}\Big|_{x=0} \qquad (3)$$

$$V_e\frac{\partial C_e}{\partial t} = -\gamma D^*\frac{\partial C}{\partial x}\Big|_{x=L} \qquad (4)$$

where V_s and V_e are the volume of source and exit reservoirs respectively, C_s and C_e are solute concentrations in source and exit reservoirs respectively, γ is the effective cross sectional area through which diffusion occurs, and L is the thickness of the porous disk.

The effective cross sectional area, γ, is described as $\gamma = An_t$ where A is the area in contact with the solute, and n_t is the effective porosity of the porous zone.

The initial conditions for (2) to (4) are:

$$C_s\,(t = 0) = C_0 \tag{5}$$

$$C_e\,(t = 0) = 0 \tag{6}$$

$$C\,(x, 0) = 0 \qquad 0 < x < L \tag{7}$$

The boundary conditions are:

$$C_s\,(t) = C\,(0, t) \tag{8}$$

$$C_e\,(t) = C\,(L, t) \tag{9}$$

3.3.1 Solution method

Equations (2), (3) and (4), subject to the initial and boundary conditions stated in equations (5) to (9), can be solved analytically by the Laplace transform method. The Laplace transformed form of the governing equations are homogenous ordinary differential equations. Equations (2), (3) and (4), therefore, transform to:

$$\frac{d^2\overline{C}}{dx^2} - \frac{s}{D^*}\overline{C} = 0 \tag{10}$$

$$sV_s\overline{C}_s - V_sC_0 = \gamma D^* \frac{d\overline{C}}{dx}\Big|_{x=0} \tag{11}$$

$$sV_e\overline{C}_e = -\gamma D^* \frac{d\overline{C}}{dx}\Big|_{x=L} \tag{12}$$

The overbar indicates the transformed form of the variable and s is the Laplace variable. The general solution to (10) is:

$$\overline{C} = A\exp(\sqrt{\frac{s}{D^*}}x) + B\exp(-\sqrt{\frac{s}{D^*}}x) \tag{13}$$

where A and B are unknown variables. By substituting (13) into (11) and (12), the following equations can be derived:

$$\overline{C}_s = \frac{(A-B)\gamma\sqrt{sD^*} + V_s C_0}{sV_s} \tag{14}$$

$$\overline{C}_e = \frac{-A\gamma\sqrt{sD^*}\exp(\sqrt{\frac{s}{D^*}}L) + B\gamma\sqrt{sD^*}\exp(-\sqrt{\frac{s}{D^*}}L)}{sV_e} \tag{15}$$

The Laplace transform is also applied to the boundary conditions. Hence, equations (8) and (9) become:

$$\overline{C}_s(s) = \overline{C}(0,s) = A + B \tag{16}$$

$$\overline{C}_e(s) = \overline{C}(L,s) = A\exp(\sqrt{\frac{s}{D^*}}L) + B\exp(-\sqrt{\frac{s}{D^*}}L) \tag{17}$$

By combining equations (14) and (15) with (16) and (17), the following set of equations can be written:

$$\gamma\sqrt{sD^*}(A-B) - sV_s(A+B) + V_s C_0 = 0 \tag{18}$$

$$\begin{aligned} &sV_e\left[A\exp(\sqrt{\frac{s}{D^*}}L) + B\exp(-\sqrt{\frac{s}{D^*}}L)\right] + A\gamma\sqrt{sD^*}\exp(\sqrt{\frac{s}{D^*}}L) \\ &- B\gamma\sqrt{sD^*}\exp(-\sqrt{\frac{s}{D^*}}L) = 0 \end{aligned} \tag{19}$$

Equations (18) and (19) are solved for unknown variables A and B. Once A and B are determined, the system is numerically inverted from the Laplace domain using the De Hoog algorithm (De Hoog et al., 1982). The De Hoog algorithm has been used successfully to invert several solute transport problems from the Laplace domain to the time domain, and has been proven to be a robust method (Novakowski and van der Kamp, 1996).

The solution scheme described above has been implemented in a FORTRAN code by Yungwirth (2006). Volumes of source and exit reservoirs, porous zone thickness, effective diffusion coefficient and porosity, initial concentration of the tracer, cross sectional area through which diffusion occurs, test time and time intervals are defined in the input file. A sample input file is shown in Appendix B. The program reads the values from the input file and creates an array of time steps at which source and exit reservoir concentrations are to be calculated. Time values are sent to a subroutine that implements the De Hoog algorithm and assigns a particular value of s. Equations (18) and (19) are then solved at this particular value to find unknown variables A and B. These variables are substituted back into (14) and (15) to calculate the concentration of source reservoir at $x = 0$ and exit reservoir at $x = L$. The concentration values at s are then returned back to the De Hoog algorithm subroutine where it is numerically inverted from the Laplace domain into the time domain. This process is repeated for each time step.

3.4 Results

3.4.1 Biofilm growth

Prior to growing the bacteria on the porous ceramic disks, preliminary efforts to optimize the growth condition on glass slides, confirmed the attachment of bacteria to glass slides. A fairly uniform biofilm was observed on glass slides left in the batch containing *E. coli* showing one layer of rod-shape bacteria distributed evenly on the glass slide. While, glass slides put in *P. putida* batch showed a comparatively denser mat of bacteria attached to the glass surface. Biofilm attachment to glass slides suggested biofilm development on the ceramic surfaces, since the relatively rough surface of ceramic was a more favourable substratum for bacteria to attach in comparison with a smooth glass surface (Scheuerman et al., 1998). A whitish slimy film, similar to that seen on the glass slides, accumulated on the surface of the ceramic disks after the growth phase. However, the presence of the surface film could not be visually seen upon disassembly of the cells once the tests were complete. However, evidences from two previous studies on the subject, indicated that a majority of the biofilm may have formed in the pores instead of on the surface (Charbonneau et al., 2006; Yungwirth, 2006).

3.4.2 Ceramic porosity

The porosity of each disk was measured upon disassembly of the diffusion cell. Although the data sheet provided by the supplier suggested an approximate value of 50% for the porosity (Soilmoisture Equipment Corp., Santa Barbara, CA, USA), the calculated total porosities were consistently equal to 61 % (±1%). This discrepancy may be due to the type

of material used in high flow ceramic disks (selected for this study) which generally consists of over 90% Alumina (Al_2O_3). Alumina has a higher density (3.97 g/cm^3) in comparison with the material used in standard disks (56% SiO_2, 15% Al_2O_3, 12% MgO, and small amounts of Fe_2O_3, CaO, TiO_2, K_2O, and Na_2O).

3.4.3 Model fitting

In order to estimate the transport properties of the porous material, the analytical model was fit to each concentration-time profile obtained from the diffusion cells. The model fitting was performed by fixing the cell geometry and disk porosity, and adjusting the model-independent parameter of effective diffusion coefficient (D^*). The free aqueous diffusion coefficient (D_0) of the tracers were used to back-calculate the tortuosity. Values found in the literature for free aqueous diffusion coefficient of Br^- were $2.01*10^{-9}$ at 25 °C as reported by Stokes (1950) and $2.08*10^{-9}$ m^2/sec ($1.8*10^{-4}$ m^2/day) reported by Lide (1992). The latter was used in this study. Free aqueous diffusion coefficient of Lissamine has been estimated as $4.5*10^{-10}$ m^2/sec ($3.9*10^{-5}$ m^2/day) by Novakowski and van der Kamp (1996). This value has not been measured directly but estimated from comparing Lissamine to Uranine, a dye with similar molecular structure to Lissamine (e.g. Skagius and Neretnieks, 1986).

To achieve the best fit, the effective diffusion coefficient was varied until the difference between the model output and experimental data was minimized. The best fit was determined by minimizing the sum of squared differences between the model and experimental data. This process was performed for Br^- profiles obtained from exit reservoirs and Lissamine profiles obtained from both source and exit reservoirs. The

effective diffusion coefficients were then used to calculate the tortuosity values using the stated free aqueous diffusion coefficients for Br^- and Lissamine. A summary of model derived tortuosity values is presented in Table 3.1. The entire cell concentration data are presented in Appendix C and the best fits to the experimental results for all cells are illustrated in Appendix D.

3.4.4 Tracer analysis

3.4.4.1 Bromide

A combination bromide electrode (Orion 9635, Thermo Electron Corporation, MA, USA) was used to detect the bromide concentration. Br^- concentration was monitored by putting the electrode into both source and exit reservoirs. The electrode was calibrated using at least five standard solutions of varying concentration between 5 and 1000 ppm before each reading. A sample calibration procedure for the bromide electrode is described in Appendix F. The initial concentration of Br^- in the source reservoirs was 1500 ppm.

The Br^- concentrations in the source and exit reservoirs were measured for the initial set of diffusion experiments. The Br^- concentrations obtained from these experiments indicated a mass build up of Br^- in all cells, even though Br^- is considered to be a conservative tracer. The background concentration was verified to be zero initially in the exit reservoirs, and the cells were built in a manner to minimize any potential leakage or evaporation. In addition, the Br^- profiles obtained for source reservoirs did not show a consistent downward trend, as predicted by the model, in many of cells. A summary of Br^- mass balances, including the minimum, maximum and the average mass balances calculated at each sampling time for

each cell, is presented in Table 3.2. It is to be mentioned that mass balances at each sampling time are calculated according to the following equation:

$$M.B. = \frac{C_s V_s + C_e V_e + \frac{(C_s + C_e)}{2} n V_d}{C_0 V_s} \tag{20}$$

where, $M.B.$ is the mass balance, and V_d is the volume of the porous disk.

The most valid hypothesis to explain these irrational findings was that the Br^- electrode did not act satisfactorily in high concentration ranges although a wide range of concentration (0.4 – 79900 ppm) has been suggested by the supplier in which the electrode was supposed to perform reliably. This hypothesis is fortified by the fact that an exponential equation was used to convert the readings in millivolt to Br^- concentration. As a result, small errors in the readings for high concentrations could cause a considerable error of Br^- concentration. Because of the uncertainty, the Br^- concentration data obtained from source reservoirs were not used to interpret the effective diffusion coefficient of the porous zone.

3.4.4.2 Lissamine

A fluorometer (Modulus, Turner BioSystems Inc., CA, USA) was used to measure the Lissamine concentration. Source reservoirs were spiked to an initial concentration of 5000 ppb and concentration was monitored for both reservoirs. The fluorometer was calibrated using at least five standard solutions of varying concentration. In total, the fluorometer was calibrated three times during the experiments.

Fitting the model to the Lissamine concentration profiles was not ideal in some cases, particularly in exit reservoir plots, and in a few cells some mass loss was observed. A summary of Lissamine mass balances, including the minimum, maximum and average mass balance calculated at the sampling time for each cell is presented in Table 3.2. In addition, the tortuosity values obtained from Lissamine profiles in exit reservoirs were up to 30% smaller than those obtained from Br^- profiles in exit reservoirs and up to 50% smaller than those obtained from Lissamine profiles in source reservoirs (see Table 3.1).

If the mass loss had occurred only in cells containing bacteria, it would have been reasonable to assume that Lissamine may have been consumed by the biofilm as a carbon source or may have adsorbed to the biomass. However, the mass loss was more severe in the control cells. Therefore, decay due to biodegradation and sorption to the biomass cannot be a valid hypothesis. On the other hand, non-conservative behaviour of Lissamine as well as potential interference with other ions and biomass have been reported in the literature. Charbonneau (2006) and Zanini et al. (1997) demonstrated non-conservative behaviour of Lissamine in radial diffusion experiments. It has also been reported that the fluorescence of Lissamine could decrease significantly in the presence of chlorine. Wilson et al. (1986) reported detectable decrease in the fluorescence of Lissamine when solutions containing 100 and 500 ppb of Lissamine and 1.0 and 5.25 ppm of chlorine were tested in a laboratory. The minimal salt solution used for this study did contain chloride ion (Appendix A). Wilson et al. (1986) also reported that the fluorescence of Lissamine was observed to increase when total organic content of the solution increased.

For this particular study, despite the instabilities observed in some cells, meaningful interpretations could be produced from the Lissamine results (as can be considered in Appendix D). The estimated tortuosity values are presented in Table 3.1 (also see Appendix D for best model fits).

3.4.5 Impacts of biofilms on matrix diffusion

Impacts of biofilms on matrix diffusion can be assessed by comparing the results obtained from biofilm cells to those of control cells. The impacts of different types of bacteria exploited to develop biofilms can also be compared. Results obtained from different tracer concentrations, as well as data collected from either source or exit reservoirs of all cells, are summarized in Table 3.1. A statistical analysis of the results is presented in Appendix E.

Results presented in Table 3.1 suggest that there is no statistical difference between the results derived from the biofilm cells and the control cells as suggested by the statistical analysis presented in Appendix E. The average of the results obtained from all the Br^- profiles ($\tau = 0.022 \pm 0.001$) does not show a statistically significant difference among all types of bacteria as well as the control cells. Yet, results obtained from the second set of experiments (indicated by the number at the right end of the cell ID) exhibit a slightly lower mean tortuosity for cells containing *P. putida* ($\tau = 0.014 \pm 0.001$) compared to *E. coli* cells ($\tau = 0.021 \pm 0.000$) and control cells ($\tau = 0.019 \pm 0.002$).

Likewise, tortuosity values estimated from Lissamine profiles in exit reservoirs suggest no statistically significant difference between the impacts of different types of biofilm ($\tau = 0.030 \pm 0.002$). The results obtained for the first two control cells indicated significant loss

of mass and hence they could not be used to estimate tortuosity values. Finally, results interpreted from Lissamine profiles in source reservoirs demonstrate no statistically significant difference between the means of the values estimated for all the three microorganisms as well as the controls ($\tau = 0.047 \pm 0.006$); yet, like Br^- results, the estimated mean tortuosity values obtained in the second set of experiments are lowest for *P. putida* ($\tau = 0.023 \pm 0.005$), and largest for the control cells ($\tau = 0.041 \pm 0.003$). It should be noted that groundwater bacteria were not examined in the second set of experiments.

Results presented in Table 3.1 also demonstrate a difference between estimated tortuosity values obtained from Lissamine profiles in exit reservoirs, Br^- profiles in exit reservoirs, and Lissamine profiles in source reservoirs. The average values of tortuosity, estimated from Br^- profiles in exit reservoirs of the biofilm cells, are approximately 76% (± 2%) of those estimated from Lissamine profiles in exit reservoirs, while these average values are almost equal for the control cells. Model derived tortuosity values from Lissamine data in exit reservoirs are also 55% (± 6%) of those obtained from Lissamine profiles in source reservoirs. The potential reasons for these observations are discussed in the following section.

3.5 Discussion

3.5.1 Biofilm growth

Biofilm development on the ceramic surfaces was supported by observing the biofilm growth on glass slides under the same growth condition as the ceramic disks, as well as direct observation of a whitish slime at the end of the growth phase. However, no biofilm

was observed on the surface of the disks, by direct visualization, after disassembly of the cells when the diffusion test was complete. Biofilm impregnation of the porous zone to a certain thickness was suggested by the previous studies on the subject (e.g. Charbonneau, 2006). Penetration of bacteria into geological material has been reported by several researchers (e.g. Escher and Characklis, 1990) and the pore size of the media used for the purpose of this study was large enough (6.0 μm) to accommodate microbial growth. However, there is no direct confirmation that the impregnation has occurred in this study. In addition, small size bacteria have often been employed in geological media. Ross et al. (2001 b), for instance, investigated the potential of ultramicrobacteria (UMB), which are defined as bacteria having a diameter smaller than 0.3 μm, to form a barrier in fractured rock. The small sizes of these bacteria, achieved upon a starvation period, improve their ability to reach small pores and fractures. The bacteria grown in this study were exposed to a very rich media in ideal growth conditions which would allow the bacteria to grow to their largest size. As a result, these microorganisms may not have penetrated into the ceramic disk; therefore, lack of biofilm growth within the porous zone is possible.

Although no carbon source was provided for the biofilm grown on the disks after they were transferred to the diffusion cells, biofilms were expected to maintain their integrity even after the carbon source was depleted, according to the results reported by Castegnier et al. (2006) who used biofilm to reduce the permeability of a fracture. Thus, it was reasonable to assume that the biofilm penetrated into the pores of the ceramic disk, it should have maintained its integrity throughout the test period. Yet, in this study it was not possible to prove the formation or survival of the biofilm by conventional microscopy method at the end of the test period.

3.5.2 Tracers' monitoring and performance

Although the bromide electrode used in this study provided a convenient method to monitor Br^- concentration, it did not perform satisfactorily at high concentrations, and did not present sensible Br^- data in the source reservoirs. A wide range of the standard solutions should have been used when calibrating the electrode to assess its performance in high concentration ranges. More reliable techniques, such as Ion Chromatography (IC), should have also been employed or serial dilution could have been done to the samples withdrawn from the source reservoirs, since the electrode presented an acceptable level of certainty in reading low concentrations. However, Br^- concentration results in exit reservoirs provided data which were consistent with the expected trends and could be used to calibrate the model, particularly at early times of the experiment. Thus, they should be good indicators of transport characteristics of the media.

Literature is inconsistent on Lissamine as a conservative tracer. Although it has been reported to behave conservatively in a number of field experiments (Novakowski and Lapcevic, 1994; van der Kamp et al., 1996), some researchers failed to generate meaningful results in tracer investigations due to unexpected fluorescence decay (Zanini et al., 1997; Charbonneau et al., 2006). Its fluorescence may also be affected by solution salinity (Smart and Laidlaw, 1977). In the case of this study, Lissamine performed reasonably well in the presence of biomaterial, while in the absence of bacteria, unexpected fluorescence decay occurred in a few cases. In the first two control cells, extensive fluorescence loss occurred to the extent that it was impossible to estimate the tortuosity values. Similarly in the exit reservoirs the model could not be fitted to the Lissamine profiles in some cells. On the

other hand, source reservoir profiles demonstrated data which were consistent with the expected trends (see Appendix D).

3.5.3 Biofilm impact on matrix diffusion

Tortuosity results were statistically analyzed for the equality of the population means (see Appendix E). Results obtained from Br^- profiles in control cells were compared to those from the biofilm-containing cells for equality of the population means. Two-tail student t-tests with 95% confidence intervals were also performed on the tortuosity data estimated from the Lissamine profiles in the source and exit reservoirs of *E. coli* and *P. putida* cells.

Analyses performed on the data suggested no statistically significant difference between the matrix diffusion values obtained from the Br^- profiles in the exit reservoirs of biofilm and control cells, as well as Lissamine profiles in source and exit reservoirs. Although results obtained from the second set of experiments indicated a slight impact of the biofilm on matrix diffusion, particularly for *P. putida* biofilm, the statistical analysis of the entire results suggested no significant impact of the biofilm.

Biofilms have heterogeneous structures mostly composed of a porous EPS matrix. Voids in the EPS matrix, usually filled with water and soluble species, facilitate flow through the system. Mass transport within biofilms is, therefore, influenced by their heterogeneity and interstitial voids distribution. In order to impede diffusion, a packed structure for the biofilm is preferred. Nutrient loading and flow condition have been previously shown to impact the biofilm structure and compactness (Jennings et al., 1995; Stoodley et al., 1999; Ross et al., 1998). Due to the very rich growth condition and moderate flow, biofilms

formed in this study should have consisted primarily of loose films rather than dense films. Furthermore, unlike small size bacteria previously used in biobarriers in fractured rocks (Ross et al., 2001b), in this study, bacteria were overloaded with nutrients, forcing them to gain their largest possible size. Considering that there was no confirmation of the existence of a biofilm at the end of the tests, it should also be taken into consideration that there may not have been any biofilm within the pores during the experiment period.

Tortuosity values obtained from Br^- profiles were up to 26% less than those estimated from Lissamine data in exit reservoirs. Considering that tortuosity is a characteristic of porous material and does not change with the tracer used for the experiments (Zanini et al., 1997), the distinction between Br^- and Lissamine derived tortuosity values may be attributed to experimental errors.

Likewise, tortuosity values estimated from Lissamine data in exit reservoirs were up to 51% less than those of source reservoirs. As can be observed in the last column of Table 3.1, there is a consistent reduction in Lissamine derived tortuosity values from source and exit reservoirs which may suggest the non-conservative behaviour of Lissamine in presence of biomaterials as suggested by Wilson et al. (1986). However, the extent and accuracy of the data obtained in this study were not sufficient enough to draw a tangible conclusion in this regard, and this distinction may also be attributed to the experimental errors.

3.5.4 Biofilm characterization

Biofilm characterization was one of the main limitations in this study. Although biofilm was observed to grow on glass slides by optical microscopy, it was not practical to observe

it directly on the surface of ceramic disks by conventional microscopy methods. In addition, ceramic disks were broken upon removal from the cells to observe the biofilm impregnated zone. However, it was not possible to observe the rough surface of the ceramic with a magnification high enough to detect bacteria or EPS structure.

Scanning electron microscopy (SEM) or an appropriate staining technique should be employed to characterize the biofilm structure and impregnated zone. Further investigation should be carried out to address these issues.

3.6 Conclusions

Biofilms were developed on ceramic disks using three types of microorganisms; *E. coli* (K12), *P. putida,* and an indigenous groundwater population. Evidence of biofilm growth was supported by detecting the biofilm grown on glass slides experiencing the same growth condition as the ceramic disks, using optical microscopy, and via visual inspection before the disks were placed in the cells. A denser film was developed by *P. putida*, compared to the thin biofilm observed on glass slides developed by *E. coli*. Biofilms were expected to maintain their integrity during the test period although there was no confirmation of the existence of the biofilm on the surface or within the porous matrix at the end of the experiments.

Model derived results for tortuosity for the biofilm stimulated disks and control disks did not suggest a significant impact of biofilm on the transport properties of the ceramic disks. This could be due to the lack of the growth or survival of biofilm on the surface or within

the pores of the disks, heterogeneity of biofilm structures, and loose structures of developed biofilms as a result of nutrient overloading.

Lissamine, used as a tracer in the diffusion experiments, did not perform as a conservative tracer in a few cells. Particularly in exit reservoirs, model output did not provide a good match to the Lissamine profiles and fluorescence decay may have occurred. A comprehensive investigation is required to characterize Lissamine behaviour in the presence of other ions, biomaterials, and non-dissolved residues.

More investigation is recommended to characterize the biofilm structure and to determine the extent it can penetrate into geological materials. Small size bacteria should be exploited in such investigations and moderate nutrient loading should be applied.

3.7 References

Beyenal, H., Lewandowski, Z. 2002. Internal and external mass transfer in biofilms grown at various flow velocities. Biotechnology Progress 18: 55–61.

Castegnier, F., Ross, N., Chapuis, R.P., Deschenes, L., Samson, R. 2006. Long-term persistence of a nutrient-starved biofilm in a limestone fracture. Water Research. 40: 925-934.

Characklis, W.G., Wilderer, P.A. 1989. Introduction. In: Structure and function of biofilms. Eds. Characklis, W.G., Wilderer, P.A. John Wiley & Sons Inc., Toronto pp. 1-4.

Charaklis, W., Marshall, K. 1990. Biofilms. John Wiley & Sons, Inc., New York, NY.

Charbonneau, A., Novakowski, K., Ross, N. 2006. The effect of a biofilm on solute diffusion in fractured porous media. Journal of Contaminant Hydrology 85: 212–228.

Crank, J. 1975. The mathematics of diffusion. Clarendon Press, Oxford, 2nd ed. 414 pp.

Davis, S.N., Campbell, D.J., Bentley, H.W., Flynn, T.J. 1985. Groundwater tracers. US Environmental Protection Agency, Oklahoma, 61-113.

de Beer, D., Stoodley, P., Roe, F., Lewandowski, Z. 1994. Effects of biofilm structures on oxygen distribution and mass transport. Biotechnology and Bioengineering 43: 1131-1138.

De Hoog, F.R., Knight, J.H., Stokes, A.N. 1982. An improved method for numerical inversion of Laplace transforms. SIAM Journal of Scientific and Statistical Computing 3(3): 357-366.

Escher, A., Characklis, W.G. 1990. Modeling the initial events in biofilm accumulation. In: Biofilms, eds. Characklis, W.G., Marshall, K.G. John Wiley & Sons, Inc., Toronto, 445-486.

Fan, L.S., Ramos, R.L., Wisecarver, K.D., Zehner, B.J. 1990. Diffusion of phenol through a biofilm grown on activated carbon particles in a draft-tube three-phase fluidized bed bioreactor. Biotechnology and Bioengineering 35: 279-286.

Gantzer, C. J., Rittmann, B.E., Herricks, E.E. 1991. Effects of long term water velocity changes on streambed biofilm activity. Water Resources 25: 15-20.

Hill, D.H., Sleep, B.E. 2002. Effects of biofilm growth on flow and transport through a glass parallel plate fracture. Journal of Contaminant Hydrology 56: 227-246.

Jennings, D.A., Petersen, J.N., Skeen, R.S., Hooker, B.S., Peyton, B.M., Johnstone, D.L., & Yonge, D.R. 1995. Effects of slight variations in nutrients loadings on pore plugging in soil columns. Applied Biochemistry and Biotechnology 51-52: 727-734.

Kemp, P.F., Sherr, B.F., Sherr, E.B., Cole, J.J. (Eds.). 1993. Handbook of methods in aquatic microbial ecology. Boca Raton, FL: Lewis Publishers.

Lawrence, J.R., Korber, D.R., Wolfaardt, G.M., Caldwell, D.E. 1995. Behavioral Strategies of Surface-Colonizing Bacteria. In: Advances in Microbial Ecology. (Eds). Jones, J.G. Plenum Press, New York, 1-76.

Leon Ohl, A., Horn, H., Hempel, D.C. 2004. Behaviour of biofilm systems under varying hydrodynamic conditions. Water Science and Technology 49(11-12): 345-51.

Mutch, R.D., Scott, J.I., Wilson, D.J. 1993. Cleanup of fractured rock aquifers: implications of matrix diffusion. Environmental Monitoring and Assessment 24: 45-70.

Novakowski K.S., van der Kamp, G. 1996. The radial diffusion method 2. A semi analytical model for the determination of effective diffusion coefficients, porosity, and adsorption. Water Resources Research. 32(6): 1823-1830.

Novakowski, K.S. 1989. A composite analytical model for analysis of pumping tests affected by wellbore storage and finite thickness skin. Water Resources Research 25(9): 1937-1946.

Novakowski, K.S. 1992. An evaluation of boundary conditions for one-dimensional solute transport 2, column experiments. Water Resources Research 28(9): 2411-2423.

Novakowski, K.S., Lapcevic, P.A. 1994. Field measurement of radial solute transport in frractured rock, Water Resources Research 30: 37-44.

Pedersen, K. 1993. The deep subterranean biosphere. Earth-Science Reviews 34: 243-260.

Pedersen, K. 2000. Exploration of deep intraterrestrial microbial life: current perspectives. FEMS Microbiology Letters 185: 9-16.

Razatos, A., Ong, Y.L., Sharma, M.M., Georgiou, G. 1998. Molecular determinants of bacterial adhesion monitored by atomic force microscopy. Proceedings of National Academy of Sciences, USA 95: 11059-11064.

Robinson, N.I., Sharp Jr., J.M., Kreisel, I. 1998. Contaminant transport in sets of parallel finite fractures with fracture skins. Journal of Contaminant Hydrology 31: 83-109.

Ross, N., Bickerton, G. 2002. Application of biobarriers for groundwater containment at fractured bedrock sites. Remediation 12 (3): 5-21.

Ross, N., Deschenes, L., Bureau, J., Clément, B., Comeau Y., Samson, R. 1998. Ecotoxicological assessment and effects of physicochemical factors on biofilm development in groundwater conditions. Environmental Science and Technology 32(8): 1105-1111.

Ross, N., Villemur, R., Deschênes, L., Samson, R. 2001. Clogging of a limestone fracture by stimulating groundwater microbes. Water Research 35: 2029-2037.

Ross, N., Villemur, R., Marcandella, É., Deschênes, L. 2001b. Assessment of changes in biodiversity when a community of ultramicrobacteria isolated from groundwater is stimulated to form a biofilm. Microbial Ecology 42: 56-68.

Rowe, R.K., Quigley, R.M., Booker, J.R. 1997. Clayey barrier systems for waste disposal facilities. E & FN Spon, New York 187-200.

Scheuerman, T.R., Camper, A.K., Hamilton, M.A. 1998. Effect of substratum topography on bacterial adhesion. Journal of Colloid Interface Science 208: 23-33.

Shackelford, C.D. 1991. Laboratory diffusion testing for waste disposal. A review. Journal of Contaminant Hydrology. 7(3): 177-217.

Siegrist, H., Gujer, W. 1985. Mass transfer mechanisms in a heterotrophic biofilm. Water Research 19(11): 1369-1378.

Skagius, K., Neretnieks, I. 1986. Porosities and diffusivities of some nonsorbing species in crystalline rocks, Water Resources Research. 22(3): 389-398.

Smart, P.L., Laidlaw, I.M.S. 1977. An evaluation of some fluorescent dyes for water tracing. Water Resources Research 13(1): 15-33.

Stokes, R.H. 1950. The diffusion coefficient of eight uni-univalent electrolytes in aqueous solution. American Chemical Society Journal 72: 2243-2247.

Stoodley, P., de Beer, D., Lewandowski, Z. 1994. Liquid flow in biofilm systems. Applied and Environmental Microbiology 60: 2711-2716.

Stoodley, P., Dodds, I., Boyle, J.D., Lappin-Scott, H.M. 1999. Influence of hydrodynamics and nutrients on biofilm structure. Journal of Applied Microbiology Symposium Supplement 85: 19S-28S.

Ude, S., Arnold, D.L., Moon, C.D., Wilson, T.T., Spiers, A.J. 2006. Biofilm formation and cellulose expression among diverse environmental Pseudomonas isolates. Environmental Microbiology Page 8(11): 1997-2011.

van der Kamp, G., van Stempvoort, D.R., Wassenaar, L.I.. 1996. The radial diffusion method, 1, using intact cores to determine isotopic composition, chemistry, and effective porosities for groundwater in aquitards. Water Resources Research 32: 1815-1822.

Van Rees, K.C.J., Sudicky, E.A., Rao, P.S.C., Reddy, K.R. 1991. Evaluation of laboratory techniques for measuring diffusion coefficients in sediments. Environmental Science and Technology 25(9):1605-1611.

Wilson, J.F. Jr., Cobb, E.D., Kilpatrick, F.A. 1986. Fluorometric procedures for dye tracing. in: USGS-TWRI Book 3, Chapter A12.

Yungwirth, G. A. 2006. The impact of biofilm on the process of back diffusion from a contaminated rock matrix . M.Sc Thesis. Queen's University, Kingston, Ontario, Canada.

Zanini, L., Novakowski, K., Bickerton, G. 1997. The radial diffusion method applied to dolostone samples from the Lockport Formation, Smithville, Ontario. NWRI Contribution No. 97-137.

Table 3.1: Summary of geometric factors estimated from the experimental results.

Cell ID	Br^--Exit		Lissamine-Exit		Lissamine-Source		$\frac{\tau_{Br-E}}{\tau_{Li-E}}$	$\frac{\tau_{Li-E}}{\tau_{Li-S}}$
	τ	Avg.	τ	Avg.	τ	Avg.		
1-Control-1	0.023	0.021	na	0.020	na	0.041	1.05	0.49
2-Control-1	0.022		na		na			
1-Control-2	0.021		0.018		0.044			
2-Control-2	0.017		0.022		0.038			
1-*Ecoli*-1	0.023	0.022	0.026	0.028	0.058	0.046	0.79	0.61
2-*Ecoli*-1	0.021		0.024		0.058			
3-*Ecoli*-1	0.023		0.030		0.058			
1-*Ecoli*-2	0.021		0.030		0.028			
2-*Ecoli*-2	0.021		0.030		0.028			
1-*Pputida*-1	0.030	0.023	0.034	0.030	0.074	0.050	0.77	0.60
2-*Pputida*-1	0.030		0.026		0.074			
3-*Pputida*-1	0.028		0.034		0.058			
1-*Pputida*-2	0.015		0.028		0.018			
2-*Pputida*-2	0.013		0.026		0.028			
1-GW-1	0.023	0.023	0.030	0.031	0.078	0.053	0.74	0.58
2-GW-1	0.023		0.034		0.038			
3-GW-1	0.023		0.030		0.042			

Note: Shaded areas indicate results from the second set of experiments.

Table 3.2: Summary of Br^- and Lissamine mass balances calculated in the experimental cells.

Cell ID	Br^- Mass balance			Lissamine Mass balance		
	Min.	Max.	Avg.	Min.	Max.	Avg.
1-Control-1	0.97	1.21	1.07	0.01	0.47	0.15
2-Control-1	0.89	1.18	1.06	0.01	0.67	0.17
1-Control-2	na	na	na	0.83	1.04	0.89
2-Control-2	na	na	na	0.87	1.07	0.96
1-*Ecoli*-1	0.97	1.65	1.32	0.83	1.08	0.95
2-*Ecoli*-1	0.94	1.65	1.33	0.60	0.83	0.72
3-*Ecoli*-1	0.95	1.68	1.35	0.84	1.11	0.97
1-*Ecoli*-2	na	na	na	1.02	1.10	1.06
2-*Ecoli*-2	na	na	na	0.96	1.09	1.04
1-*Pputida*-1	1.11	1.65	1.41	0.76	1.11	0.92
2-*Pputida*-1	1.07	1.68	1.40	0.74	1.03	0.89
3-*Pputida*-1	0.96	1.61	1.35	0.78	1.10	1.01
1-*Pputida*-2	na	na	na	0.99	1.09	1.06
2-*Pputida*-2	na	na	na	0.95	0.97	1.02
1-GW-1	1.08	1.32	1.16	0.81	1.02	0.92
2-GW-1	1.08	1.25	1.16	0.88	1.10	1.02
3-GW-1	1.07	1.27	1.15	0.83	1.08	0.99

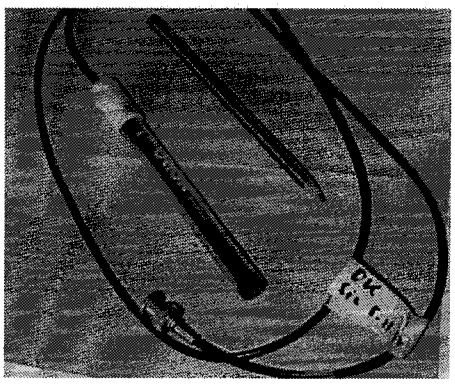

Figure 3.1: Combination bromide electrode

Figure 3.2: Fluorormeter

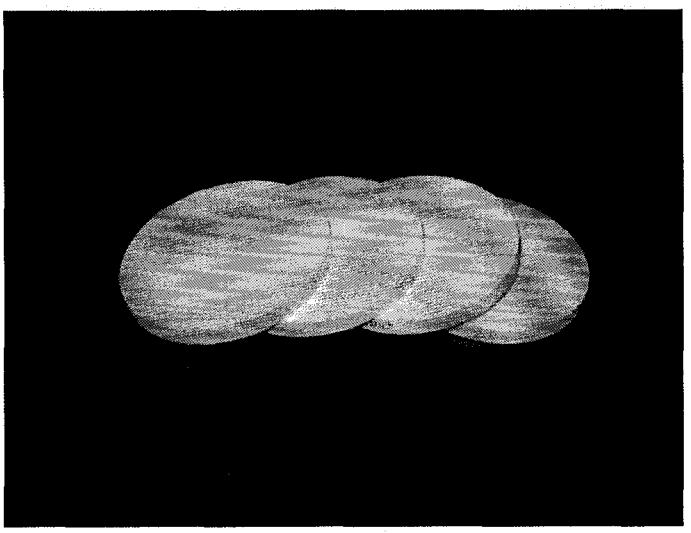

Figure 3.3: Ceramic disks

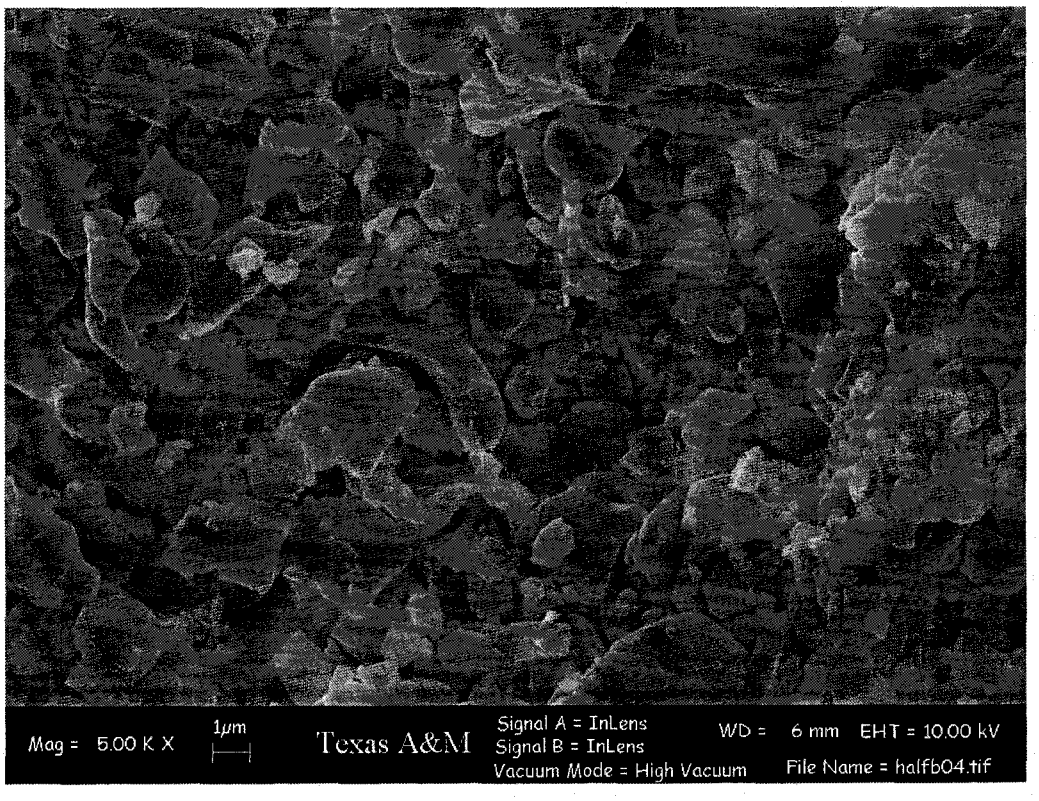

Figure 3.4: SEM image of the ceramic disk disks (Soilmoisture Equipment Corp., Santa Barbara, CA, USA)

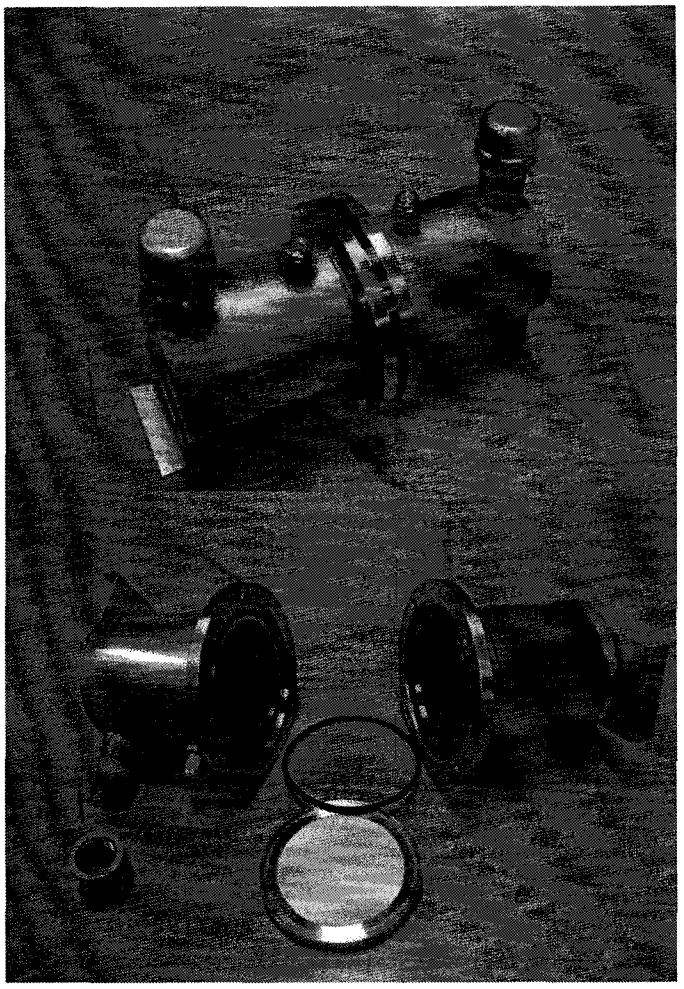

Figure 3.5: Stainless steel double-reservoir diffusion cells

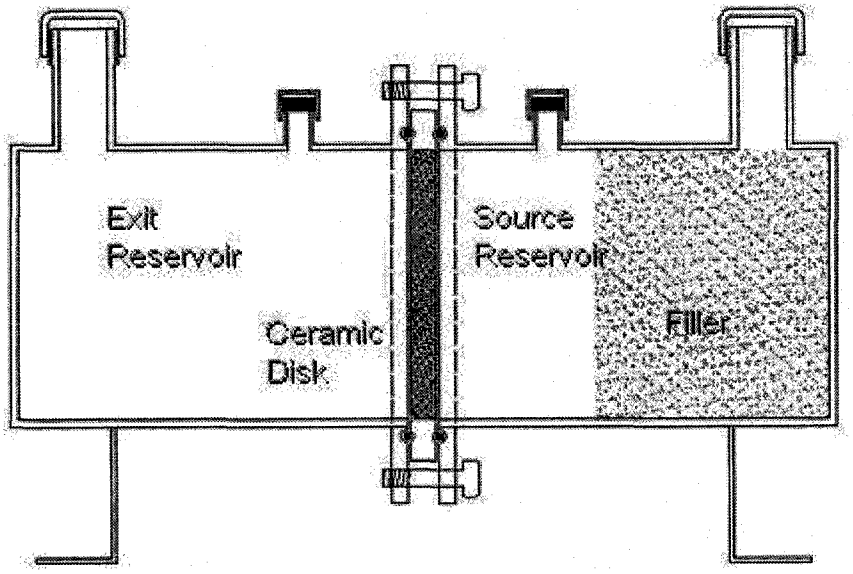

Figure 3.6: Schematic diagram of the diffusion cell

*Source and exit reservoir diameter: ~80 mm

Source and exit reservoir length: ~120 mm

Depth of occupied volume by filler material: ~85 mm

Figure 3.7: Biofilm growth batch

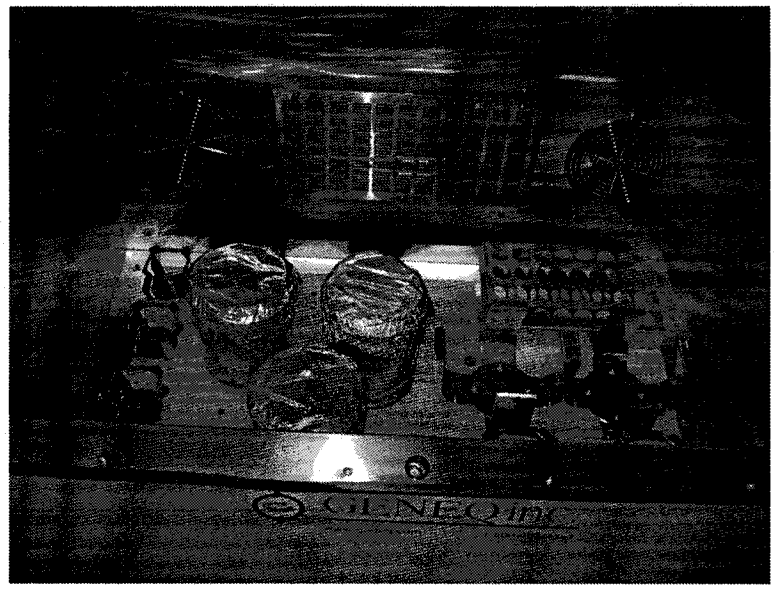

Figure 3.8: Growth batches on the rotating table

Figure 3.9: Filler material used to reduce the source reservoir volume

4 GENERAL CONCLUSIONS AND RECOMMENDATIONS FOR FUTURE STUDIES

The objective of this study was to assess the potential of a biofilm to reduce the diffusion between the rock matrix and the fracture network. Specific objectives also included comparing the impacts of different types of microorganisms, which produced different amounts of EPS, on the diffusion through the biofilm and the impregnated porous matrix.

Three species of microorganisms were exploited to form a biofilm on ceramic disks: *Pseudomonas putida*, which excrete considerable amounts of EPS, and hence develops a uniform biofilm; *Escherichia coli* (K12) that produces less EPS; and an indigenous groundwater population. Biofilm growth on ceramic disks was supported by monitoring the biofilm growth on glass slides, experiencing the same conditions as applied to the disks, as well as visualization of a whitish slime formed on the disks at the end of the growth period. Biofilm growth was expected to penetrate into the porous matrix based on the studies of Charbonneau et al. (2006) and Yungwirth (2006). In addition, biofilms were expected to maintain their integrity during the test period based on the work presented by Castegnier et al. (2006). In total, seventeen double reservoir diffusion experiments were completed, of which four cells acted as controls, five cells with *E. coli* biofilm, five cells with *P. putida* biofilm, and three cells with biofilm developed using an indigenous groundwater population. Diffusion was established across the ceramic disks by spiking the source reservoirs with two types of tracer, bromide and Lissamine, to initial concentrations of 1500 ppm and 5000 ppb respectively.

A semi-analytical model was employed to interpret the transport properties of the porous zone from the experimental data. The model was solved in the Laplace domain and a numerical approach was used to invert Laplace variables into the time domain. The model was coded in FORTRAN, and the effective diffusion coefficient term was adjusted to fit to the experimental data. The tortuosity was derived based on assumed values of the free aqueous diffusion coefficient found in the literature.

Results obtained by fitting the model to the experimental data suggested that the biofilm had no statistically significant impact on the diffusion through the ceramic disks, although the mean tortuosity values for *P. putida* biofilm experiments indicated a slight impact on the effective diffusion coefficient. This lack of significant impact of biofilm could possibly be due to the lack of sufficient biofilm growth within the pores, biofilm decay/detachment during the test period, the heterogeneity of biofilm structures, or highly porous structures of developed biofilms. The estimated tortuosity values based on the exit reservoir data for bromide were consistently 21 to 26% lower than the values estimated for Lissamine in cells where a biofilm was assumed to be present. In addition, for Lissamine, the estimated tortuosity values based on the data collected in the exit reservoirs were consistently 39 to 51% lower than the values based on the source reservoir. The potential reason for this difference may be related to the non-conservative behaviour of the Lissamine, however, this could not be confirmed and the differences may also be impacted by experimental error.

Model output did not match ideally to the Lissamine profiles in exit reservoirs in some cases. Significant Lissamine mass losses were also observed in a few cases suggesting that the Lissamine fluorescence could have been affected by other ions or residues in the solution.

Future studies on the subject should focus on the following issues:

- It is strongly recommended to characterize the biofilm structure grown on the surface of the porous material, or penetrating into the pores. The extent to which a biofilm can penetrate into a porous matrix should be investigated employing suitable microscopy techniques along with appropriate staining methods in a way not to disturb the original biofilm structure.

- It is recommended to adjust the nutrient loading, the hydrodynamic conditions, the growth period, temperature, and other environmental factors in order to obtain a more packed structure for the biofilm. It is also recommended to exploit small size bacteria, able to penetrate to a higher fraction of pores and fractures. Finally, a continuously fed reactor is more favourable for the biofilm growth compared to a batch reactor.

- Real contaminants are suggested to be utilized in similar experiments to examine the degrading ability of the biofilm and its performance as a biofilter.

- It is recommended to develop a multi-layer model to more precisely simulate the problem. Particularly, in cases where the biofilm impregnated zone is determined using suitable techniques, the multi-layer model can improve the accuracy of the results.

- It is strongly recommended to perform a thorough evaluation of Lissamine behaviour as a tracer. Its performance in the presence of other ions, biomaterial, and residues should be examined. Its potential adsorption to the geological materials should also be evaluated.

Appendix A: Minimal salt solution recipe

The minimal salt solution recipe is derived form M9 solution, a minimal growth media, excluding its carbon source (glucose). M9 contains the necessary salts at minimum concentration required for the bacterial growth. The recipe for 100 ml of minimal salt solution is as follows:

97.9 ml of sterile distilled de-ionized (DDI) water

1 ml of 10× salts stock solution

1 ml of 3000 ppm sodium nitrate stock solution

100 µl of 1M $MgSO_4$

Table A1: Chemical composition of the minimal salt solution

Components	Concentration (moles/L)
Na^+	1.707×10^{-3}
PO_4^{3-}	2.699×10^{-4}
K^+	2.205×10^{-4}
Cl^-	2.745×10^{-3}
NH_4^+	1.865×10^{-3}
Ca^{2+}	1.000×10^{-4}
NO_3^-	4.837×10^{-4}
Mg^{2+}	1.001×10^{-3}
SO_4^{2-}	1.001×10^{-3}
pH	7.00

The minimal salt solution was prepared by adding 97.9 ml of DDI water to a 150 ml flask and autoclaving it at 121°C for 20 minutes. Once at room temperature, in a sterile

environment, 1ml of 10× salts, and $NaNO_3$ stock solutions were added individually using a 3 ml non-latex syringe with 0.20 Acrodisk 32 mm filter. A precision 100 µl pipette and sterile pipette tip was used to dispense exactly 100 µl of 1M $MgSO_4$. After the addition of each ingredient, the mouth of the flask was sterilized by flame.

A.1 Preparation of 10x salts stock solution

To prepare the 10× salts stock solution, 12 g of Na_2HPO_4, 6 g of KH_2PO_4, 1 g of NaCl and 2g of NH_4Cl were weighed out to three decimal places using a precision analytical balance and dissolved in 180 ml of DDI water. The solution was autoclaved at 121°C for 20 minutes. When the solution returned to room temperature, 20ml of a 0.01M $CaCl_2$ solution were added using a 20 ml non-latex syringe with a 0.20 µm Acrodisk syringe filter. The stock solutions were all stored at 4°C.

A.2 Preparation of $NaNO_3$ stock solution

The desired concentration of $NaNO_3$ in the minimal salt solution was approximately 30 mg/L. Therefore it was necessary to make a solution of 3000 mg/L so that when 1 ml was added to a 100ml volume the concentration remained 30 ml/L. 0.3 g of $NaNO_3$ was weighed out using a precision analytical balance and placed in a 100 ml volumetric flask. DDI water was added to the line using a squirt bottle. The solution was inverted several times to mix.

A.3 Preparation of 1M $MgSO_4$ stock solution

6.01 g of $MgSO_4$ was weighed out using a precision analytical balance and placed in a 25 ml volumetric flask. DDI water was added to the line using a squirt bottle. The solution was inverted several times to mix.

Appendix B: Sample input file

Input Variables for Diffusion Cell Solution

180E-6	VIN: Volume of Source Reservoir [L^3] (m^3)
610E-6	VEX: Volume of Exit Reservoir [L^3] (m^3)
0.0071	HL: Coupon Thickness [L] (m)
5000	CO: Initial Concentration in Source Reservoir [M/L^3]
7.02E-7	DSTAR: Effective Diffusion Coefficient [L^2/T] (m^3/hr)
4.951E-3	AREA: Cross Sectional Area through which Diffusion Occurs [L^2] (m^2)
0.61	XPOR: Porosity of Geological Medium [dim]
10E-6	ERROR: Error Tollerance for DeHoog Inversion
0.0	ALPHA: Error Term DeHoog Inversion
0.8	TFACT: Time Term for DeHoog Inversion
16.0	NTERM: Number of Terms in Series for DeHoog Inversion
300	TIME: Time of Simulation[T] (hr)
50	NSTEPS: Number of Time Steps

Appendix C: Cell concentration data

Table C1: Cell concentration data

1-Control-1				
	Source reservoir		Exit reservoir	
Time (hours)	Br^- C/C_0	Lissamine C/C_0	Br^- C/C_0	Lissamine C/C_0
19.5	0.938	0.445	0.049	0.009
44.0	0.863	0.221	0.110	0.016
71.5	0.909	0.305	0.139	0.009
94.8	0.772	0.235	0.170	0.012
123.5	0.800	0.208	0.223	0.007
144.0	0.725	0.166	0.241	0.006
164.8	0.697	0.136	0.249	0.005
191.0	0.700	0.113	0.317	0.015
218.0	0.699	0.105	0.365	0.004
243.5	0.690	0.101	0.392	0.006
266.5	0.699	0.084	0.365	0.003
315.5	0.667	0.054	0.433	0.011

2-Control-1				
	Source reservoir		Exit reservoir	
Time (hours)	Br^- C/C_0	Lissamine C/C_0	Br^- C/C_0	Lissamine C/C_0
19.5	0.973	0.648	0.063	0.006
44.0	0.901	0.517	0.085	0.010
71.5	0.915	0.405	0.166	0.009
94.8	0.769	0.289	0.169	0.009
123.5	0.784	0.179	0.232	0.016
144.0	0.672	0.114	0.221	0.008
164.8	0.633	0.091	0.236	0.011
191.0	0.700	0.055	0.311	0.016
218.0	0.735	0.029	0.335	0.008
243.5	0.719	0.025	0.375	0.008
266.5	0.651	0.018	0.350	0.006
315.5	0.675	0.014	0.409	0.008
356.0	0.693	0.014	0.455	0.006

1-Control-2				
	Source reservoir		Exit reservoir	
Time (hours)	Br^- C/C_0	Lissamine C/C_0	Br^- C/C_0	Lissamine C/C_0
4.0	na	0.932	0.007	0.006
7.9	na	0.854	0.012	0.005
22.4	na	0.770	0.036	0.013
29.7	na	0.748	0.054	0.016
52.2	na	0.770	0.094	0.024
101.2	na	0.689	0.131	0.045
145.9	na	0.560	0.149	0.064
198.0	na	0.541	0.237	0.073
269.9	na	0.439	0.241	0.098
341.7	na	0.395	0.300	0.122
458.7	na	0.337	0.315	0.136

2-Control-2				
	Source reservoir		Exit reservoir	
Time (hours)	Br^- C/C_0	Lissamine C/C_0	Br^- C/C_0	Lissamine C/C_0
4.0	na	0.947	0.004	0.008
7.9	na	0.876	0.009	0.002
22.4	na	0.842	0.031	0.022
29.7	na	0.765	0.045	0.008
52.2	na	0.824	0.068	0.020
101.2	na	0.693	0.125	0.048
145.9	na	0.599	0.149	0.064
198.0	na	0.585	0.182	0.094
269.9	na	0.543	0.185	0.123
341.7	na	0.437	0.220	0.141
458.7	na	0.381	0.241	0.149

1-*Ecoli*-1				
	Source reservoir		Exit reservoir	
Time (hours)	Br^- C/C_0	Lissamine C/C_0	Br^- C/C_0	Lissamine C/C_0
15.5	0.912	na	0.032	0.025
43.0	1.003	0.921	0.106	0.090
66.3	0.826	0.879	0.135	0.098
95.0	0.816	0.911	0.204	0.135
115.5	0.809	0.823	0.225	0.105
136.3	0.807	0.827	0.213	0.115
162.5	0.923	0.756	0.313	0.118
189.5	0.923	0.785	0.361	0.128
215.0	0.990	0.783	0.451	0.152
238.0	0.877	0.749	0.463	0.154
287.0	1.038	0.747	0.570	0.199
327.5	0.937	0.703	0.616	0.171
403.5	0.871	0.669	0.661	0.202
474.5	0.866	0.643	0.711	0.210
526.0	0.788	0.595	0.692	0.212
573.5	0.707	na	0.599	0.265
645.0	0.687	na	0.613	0.290
689.7	0.722	na	0.657	0.284

2-*Ecoli*-1				
	Source reservoir		Exit reservoir	
Time (hours)	Br^- C/C_0	Lissamine C/C_0	Br^- C/C_0	Lissamine C/C_0
15.5	0.887	0.955	0.030	0.052
43.0	0.938	0.944	0.093	0.062
66.3	0.960	0.922	0.119	0.069
95.0	0.938	0.889	0.191	0.084
115.5	0.883	0.915	0.207	0.105
136.3	0.880	0.865	0.200	0.090
162.5	1.001	0.789	0.291	0.096
189.5	0.985	0.815	0.323	0.109
215.0	0.981	0.773	0.438	0.108
238.0	0.983	0.757	0.468	0.120

287.0	1.025	0.705	0.580	0.142
327.5	0.880	0.679	0.651	0.146
403.5	0.908	0.602	0.698	0.143
474.5	0.873	0.548	0.717	0.157
526.0	0.801	0.537	0.669	0.176
573.5	0.681	0.609	0.535	0.190
645.0	0.655	0.616	0.495	0.204
689.7	0.715	0.580	0.549	0.194

3-*Ecoli*-1

	Source reservoir		Exit reservoir	
Time (hours)	Br^- C/C_0	Lissamine C/C_0	Br^- C/C_0	Lissamine C/C_0
15.5	0.894	0.935	0.033	0.061
43.0	0.987	0.950	0.099	0.079
66.3	0.927	na	0.139	0.092
95.0	0.927	0.901	0.203	0.108
115.5	0.843	0.838	0.237	0.123
136.3	0.836	0.845	0.223	0.134
162.5	0.931	0.770	0.325	0.130
189.5	0.905	0.764	0.370	0.158
215.0	0.994	0.775	0.477	0.166
238.0	0.887	0.725	0.497	0.146
287.0	1.012	0.704	0.607	0.201
327.5	0.977	0.667	0.656	0.195
403.5	0.912	0.633	0.658	0.225
474.5	0.895	na	0.699	0.241
526.0	0.785	na	0.695	0.225
573.5	0.684	0.574	0.579	0.265
645.0	0.679	0.521	0.615	0.266
689.7	0.709	0.527	0.651	0.277

1-*Ecoli*-2				
	Source reservoir		Exit reservoir	
Time (hours)	Br^- C/C_0	Lissamine C/C_0	Br^- C/C_0	Lissamine C/C_0
4.4	na	0.959	0.003	0.019
19.7	na	0.875	0.027	0.036
47.7	na	0.838	0.069	0.054
73.4	na	0.817	0.131	0.057
99.2	na	0.800	0.151	0.073
122.7	na	0.777	0.178	0.088
164.8	na	0.682	0.200	0.100
216.7	na	0.652	0.205	0.115
291.7	na	0.531	0.210	0.141

2-*Ecoli*-2				
	Source reservoir		Exit reservoir	
Time (hours)	Br^- C/C_0	Lissamine C/C_0	Br^- C/C_0	Lissamine C/C_0
4.4	na	0.961	0.003	0.013
19.7	na	0.950	0.025	0.023
47.7	na	0.924	0.079	0.036
73.4	na	0.826	0.115	0.048
99.2	na	0.786	0.131	0.060
122.7	na	0.760	0.177	0.076
164.8	na	0.647	0.195	0.086
216.7	na	0.608	0.203	0.118
291.7	na	0.551	0.217	0.143

1-*Pputida*-1				
	Source reservoir		Exit reservoir	
Time (hours)	Br^- C/C_0	Lissamine C/C_0	Br^- C/C_0	Lissamine C/C_0
27.5	1.007	0.954	0.067	0.111
48.0	0.979	0.911	0.133	0.117
68.8	0.980	0.872	0.141	0.128
95.0	1.112	0.826	0.251	0.141
122.0	1.087	0.796	0.309	0.141
147.5	1.129	0.811	0.385	0.151
170.5	0.983	0.717	0.414	0.155
219.5	1.065	0.739	0.499	0.186
260.0	1.037	0.697	0.566	0.181
336.0	0.908	0.630	0.629	0.196
407.0	0.884	0.540	0.673	0.206
458.5	0.805	0.547	0.631	0.204
506.0	0.751	0.633	0.515	0.251
577.5	0.685	0.528	0.527	0.252
622.2	0.735	0.498	0.619	0.238

2-*Pputida*-1				
	Source reservoir		Exit reservoir	
Time (hours)	Br^- C/C_0	Lissamine C/C_0	Br^- C/C_0	Lissamine C/C_0
27.5	0.979	0.904	0.059	0.095
48.0	0.968	0.837	0.113	0.101
68.8	0.939	0.861	0.133	0.105
95.0	1.158	0.809	0.257	0.105
122.0	1.105	0.816	0.297	0.121
147.5	1.166	0.757	0.373	0.125
170.5	1.003	0.758	0.409	0.084
219.5	1.106	0.743	0.502	0.177
260.0	1.067	0.713	0.561	0.171
336.0	0.889	0.617	0.581	0.179
407.0	0.884	0.533	0.661	0.189
458.5	0.785	0.550	0.623	0.179
506.0	0.723	0.628	0.559	0.216
577.5	0.675	0.586	0.581	0.237
622.2	0.695	0.508	0.611	0.215

3-*Pputida*-1				
	Source reservoir		Exit reservoir	
Time (hours)	Br^- C/C_0	Lissamine C/C_0	Br^- C/C_0	Lissamine C/C_0
27.5	0.873	1.002	0.062	0.078
48.0	0.945	0.972	0.114	0.091
68.8	0.935	1.002	0.129	0.122
95.0	1.099	0.917	0.239	0.107
122.0	1.047	0.920	0.307	0.128
147.5	1.074	0.907	na	0.149
170.5	0.972	0.755	0.384	0.150
219.5	1.069	na	0.499	0.187
260.0	1.007	0.781	0.541	0.175
336.0	0.882	0.616	0.569	0.201
407.0	0.855	0.703	0.629	0.232
458.5	0.771	0.669	0.603	0.222
506.0	0.678	na	0.527	0.244
577.5	0.657	0.671	0.573	0.262
622.2	0.689	0.506	0.572	0.253

1-*Pputida*-2				
	Source reservoir		Exit reservoir	
Time (hours)	Br^- C/C_0	Lissamine C/C_0	Br^- C/C_0	Lissamine C/C_0
4.6	na	0.981	0.003	0.008
19.9	na	0.965	0.017	0.011
47.9	na	0.940	0.050	0.028
73.6	na	0.890	0.100	0.042
99.4	na	0.779	0.105	0.053
122.9	na	0.759	0.147	0.076
165.0	na	0.717	0.183	0.099
216.9	na	0.689	0.190	0.110
291.9	na	0.636	0.188	0.128

2-*Pputida*-2				
	Source reservoir		Exit reservoir	
Time (hours)	Br^- C/C_0	Lissamine C/C_0	Br^- C/C_0	Lissamine C/C_0
4.6	na	0.968	0.003	0.016
19.9	na	0.880	0.014	0.025
47.9	na	0.839	0.052	0.039
73.6	na	0.782	0.075	0.057
99.4	na	0.739	0.094	0.052
122.9	na	0.698	0.149	0.080
165.0	na	0.660	0.149	0.091
216.9	na	0.637	0.164	0.115
291.9	na	0.581	0.191	0.136

1-GW-1				
	Source reservoir		Exit reservoir	
Time (hours)	Br^- C/C_0	Lissamine C/C_0	Br^- C/C_0	Lissamine C/C_0
4.5	1.061	0.931	0.003	0.024
8.4	1.042	0.895	0.011	0.062
22.9	1.032	0.890	0.053	0.055
30.2	1.049	0.879	0.060	0.061
52.7	1.049	0.914	0.095	0.075
101.7	0.981	0.830	0.205	0.088
146.4	0.995	0.762	0.285	0.093
198.5	0.845	0.707	0.305	0.117
270.4	0.763	0.653	0.392	0.187
342.2	0.715	0.609	0.423	0.210
459.2	0.641	0.559	0.447	0.229

2-GW-1				
	Source reservoir		Exit reservoir	
Time (hours)	Br^- C/C_0	Lissamine C/C_0	Br^- C/C_0	Lissamine C/C_0
4.5	1.049	0.955	0.004	0.031
8.4	1.041	0.944	0.011	0.047
22.9	1.054	0.922	0.044	0.060
30.2	1.022	0.889	0.061	0.077
52.7	0.994	0.915	0.094	0.093
101.7	0.947	0.865	0.196	0.108
146.4	0.949	0.789	0.267	0.128
198.5	0.826	0.815	0.327	0.152
270.4	0.749	0.773	0.403	0.178
342.2	0.694	0.757	0.504	0.192
459.2	0.661	0.705	0.541	0.203

3-GW-1				
	Source reservoir		Exit reservoir	
Time (hours)	Br^- C/C_0	Lissamine C/C_0	Br^- C/C_0	Lissamine C/C_0
4.5	1.055	0.969	0.005	0.021
8.4	1.028	1.013	0.014	0.041
22.9	1.034	0.943	0.047	0.053
30.2	1.009	0.969	0.066	0.066
52.7	0.981	0.947	0.099	0.082
101.7	0.897	0.897	0.197	0.100
146.4	0.928	0.822	0.307	0.124
198.5	0.793	0.799	0.327	0.136
270.4	0.729	0.767	0.405	0.169
342.2	0.685	0.726	0.503	0.184
459.2	0.629	0.599	0.506	0.203

Appendix D: Concentration profiles and the best fits

Figure D1: Plots of concentration vs. time and the best fits*

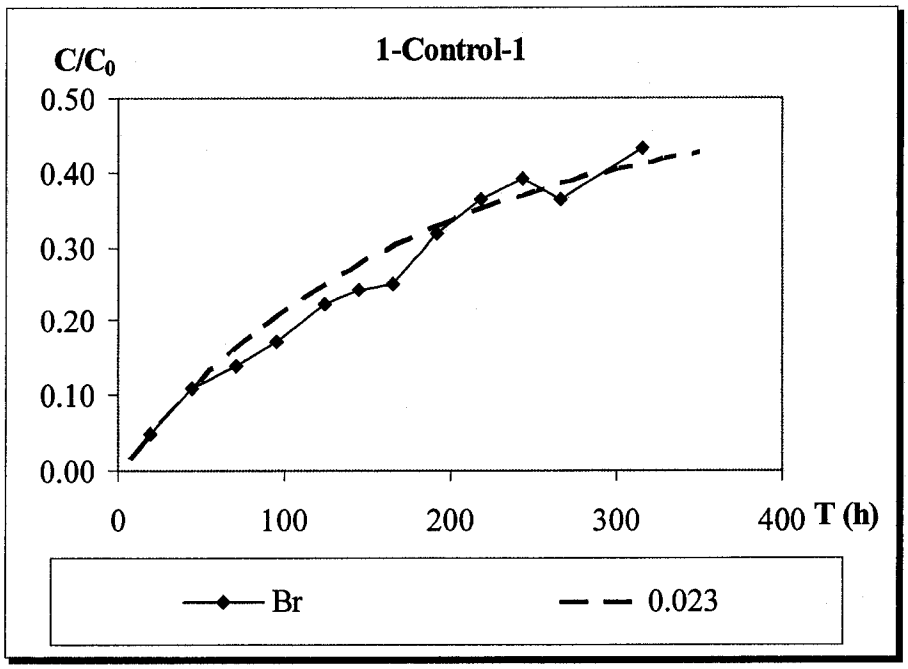

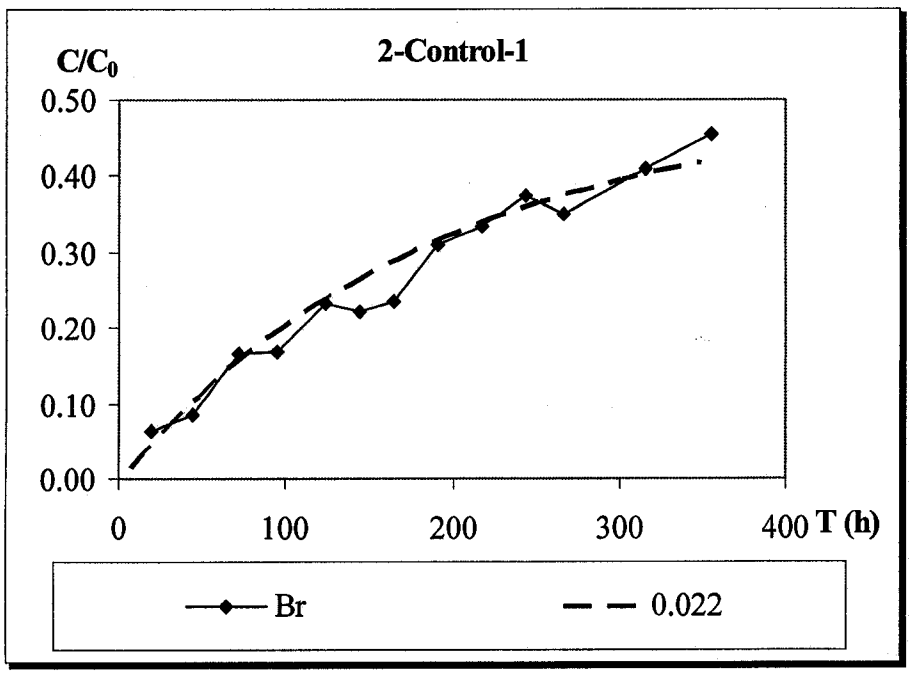

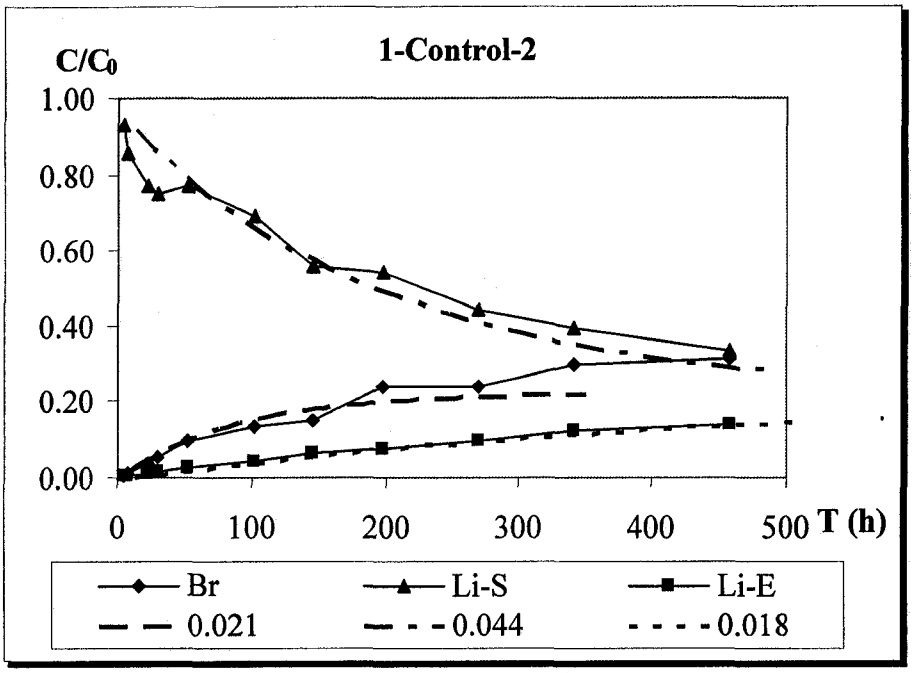

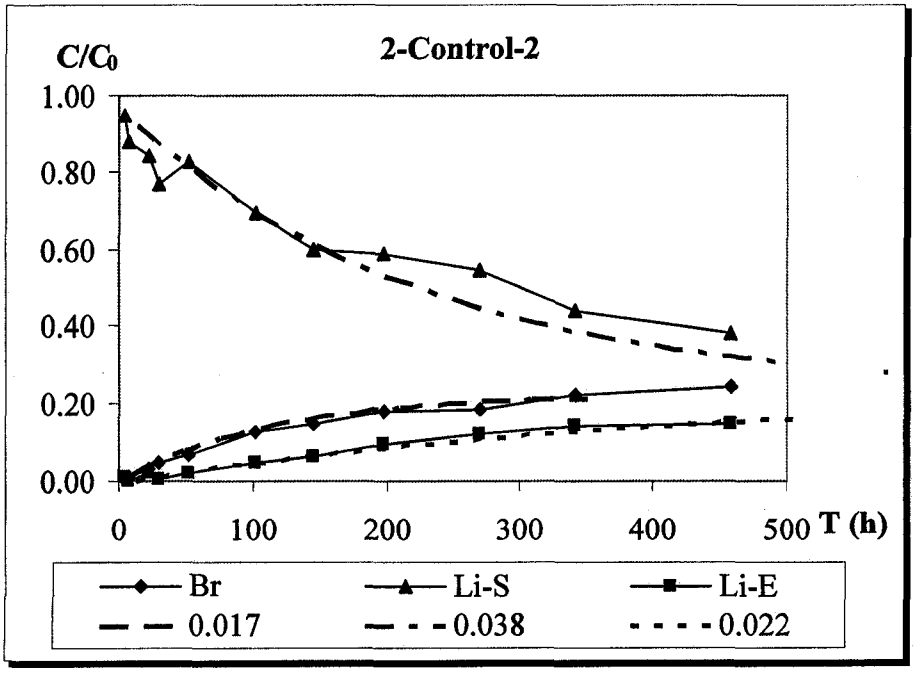

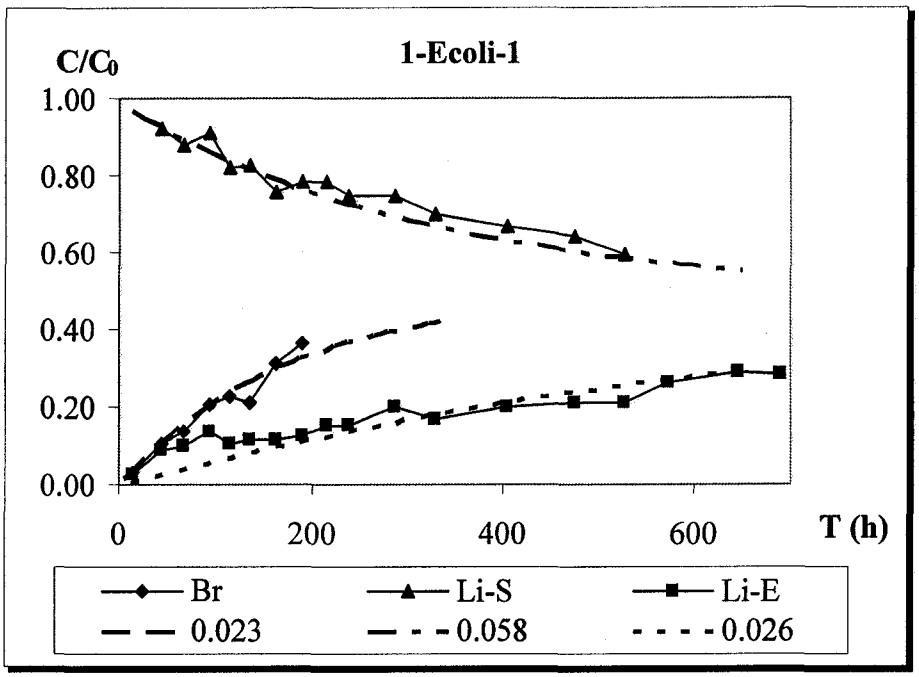

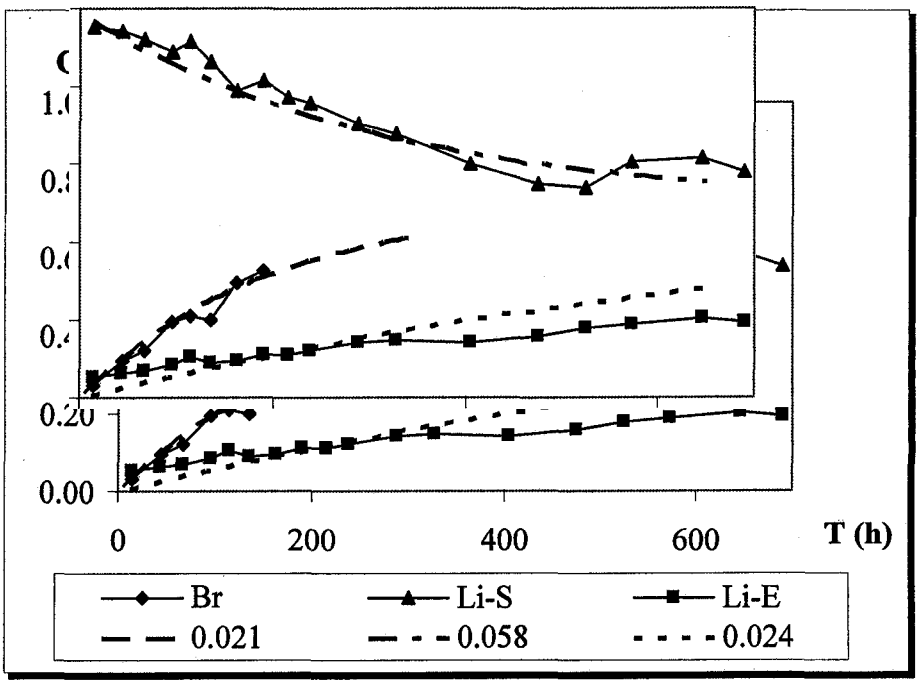

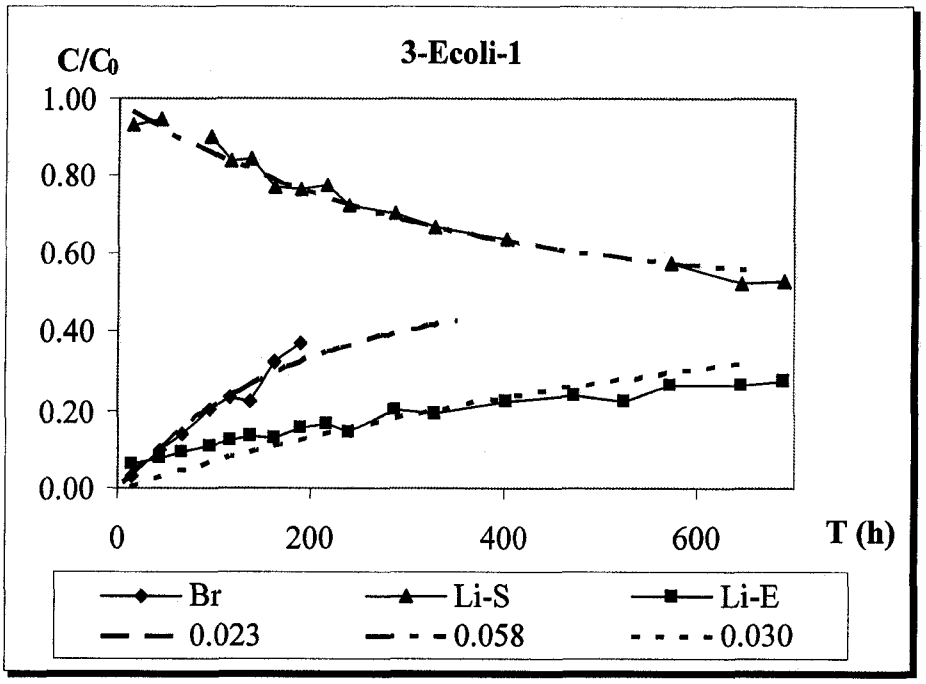

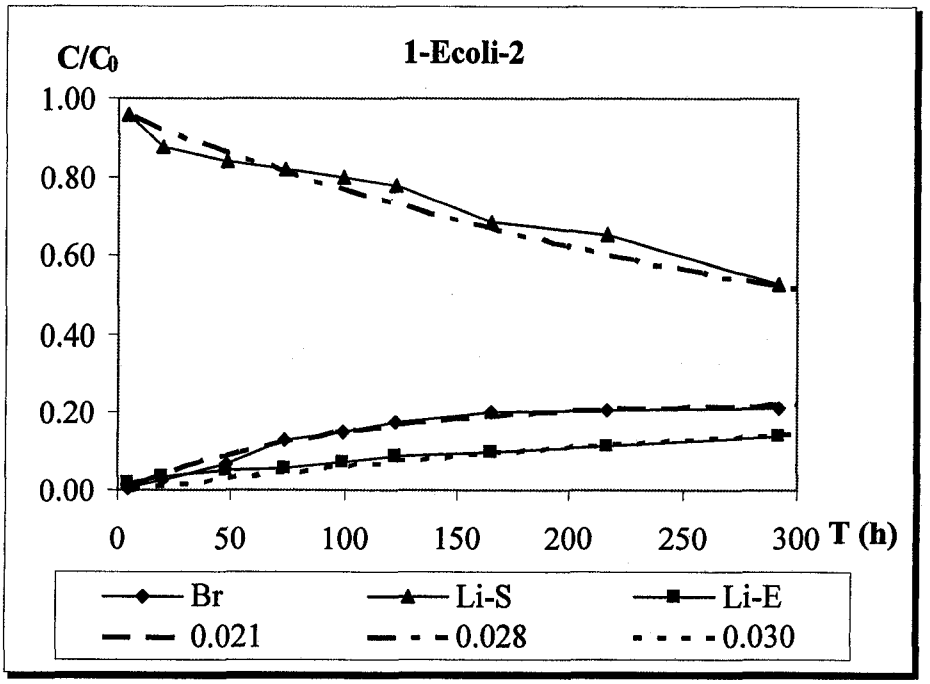

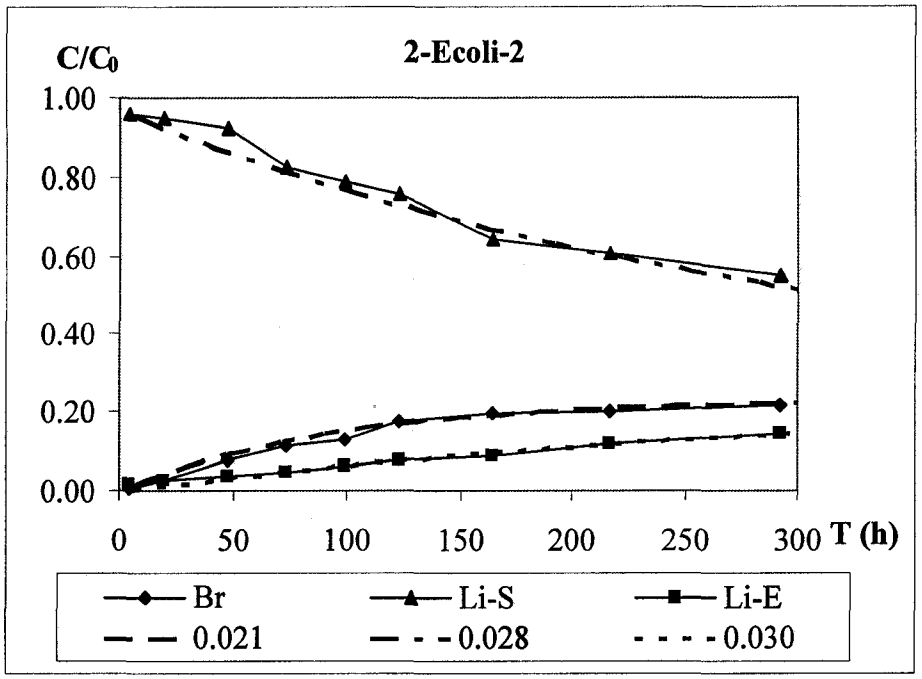

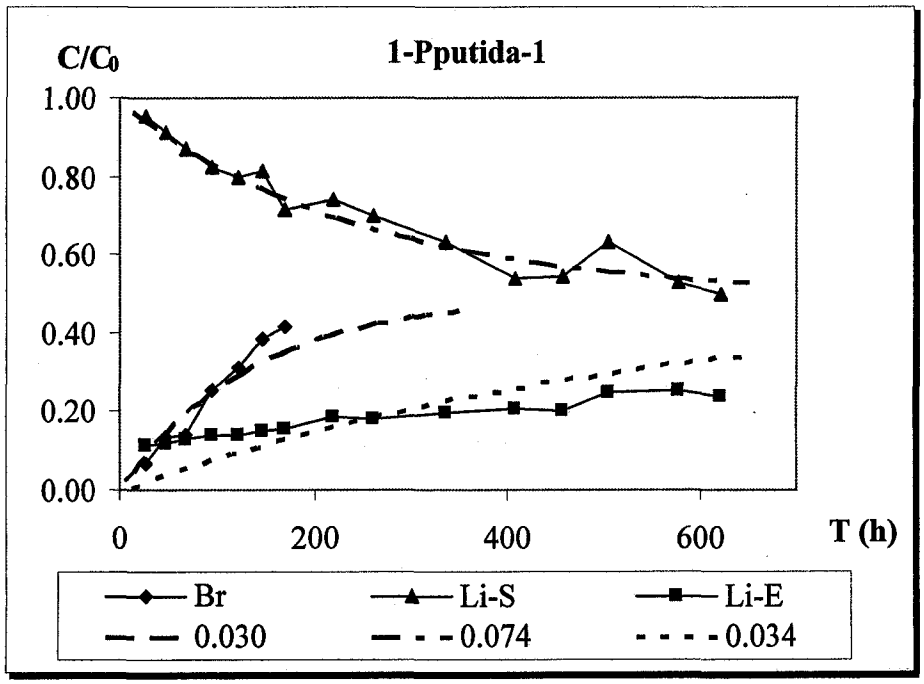

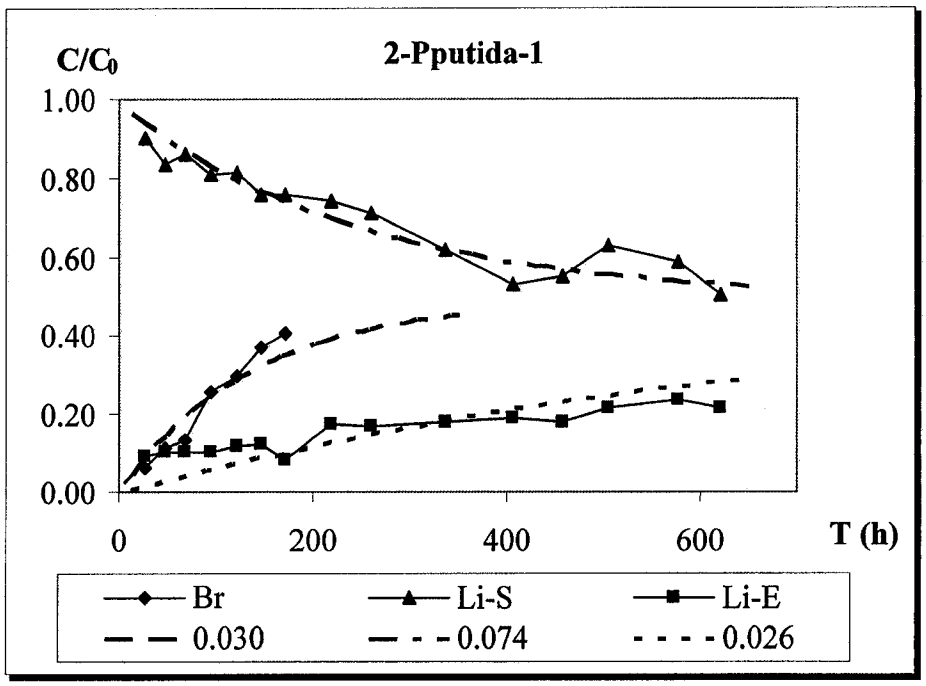

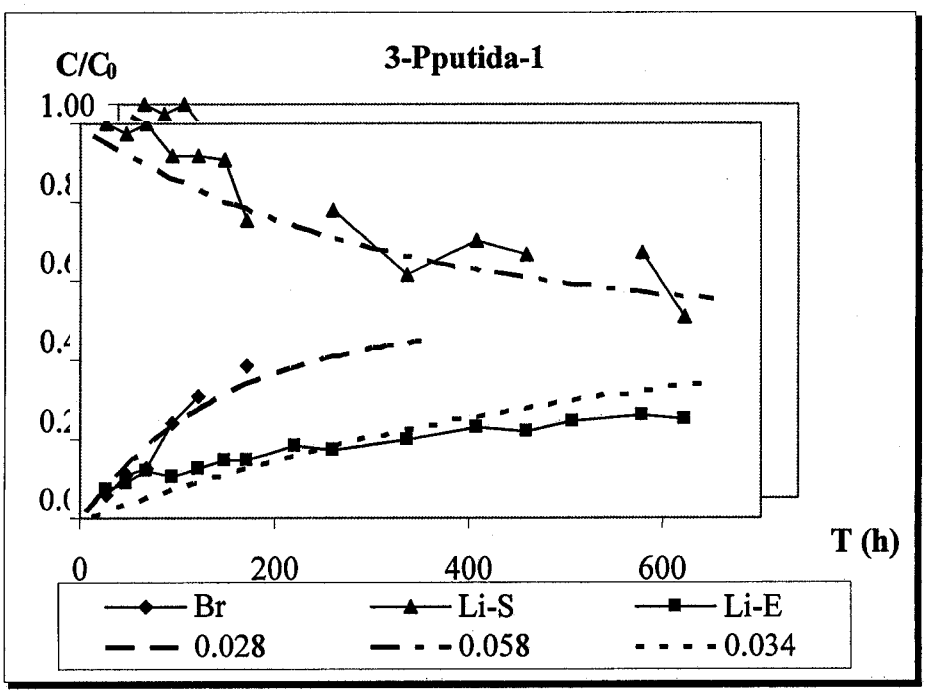

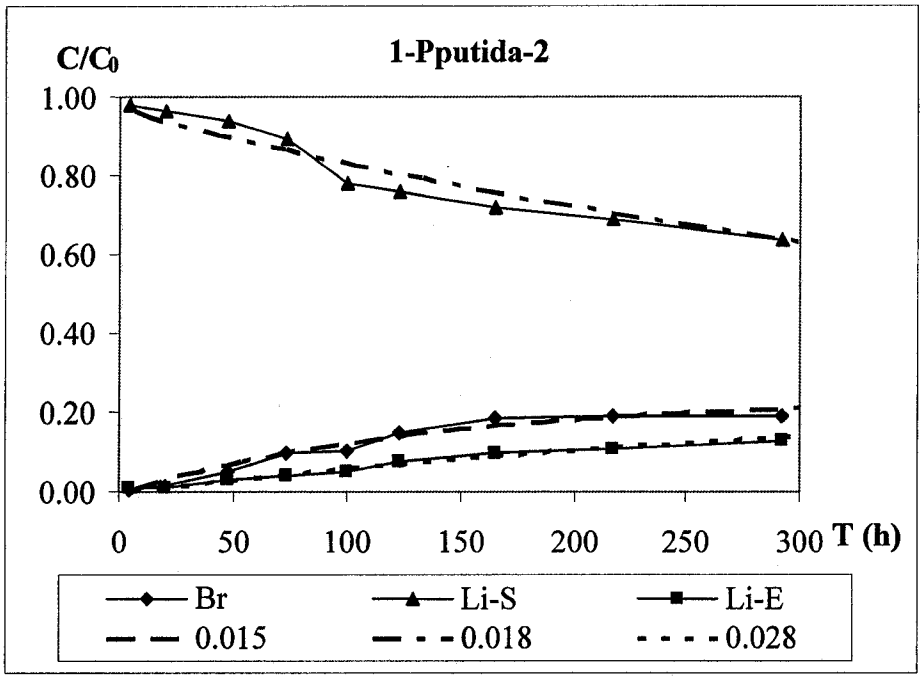

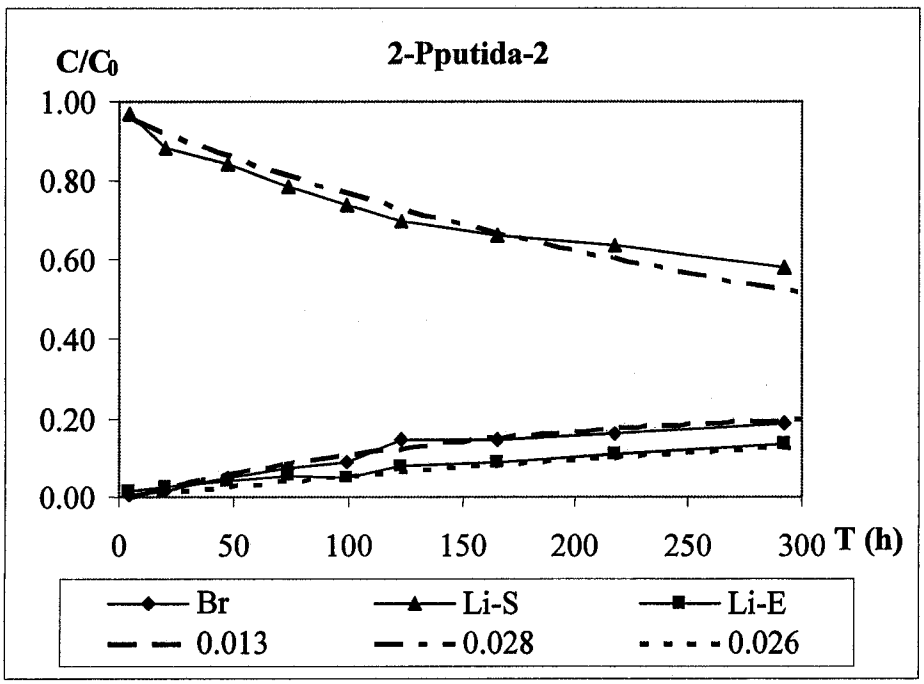

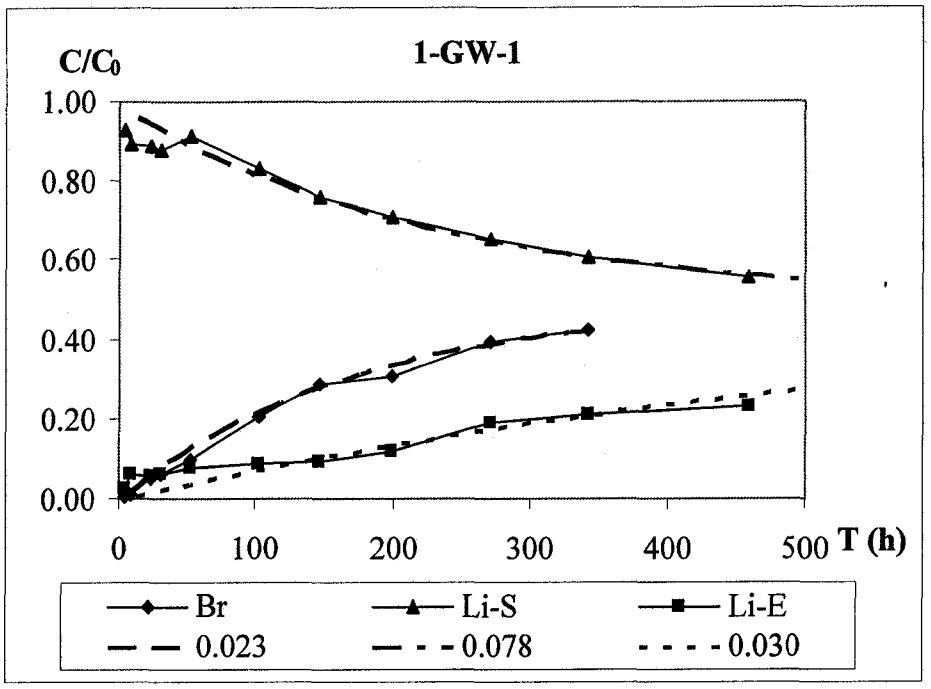

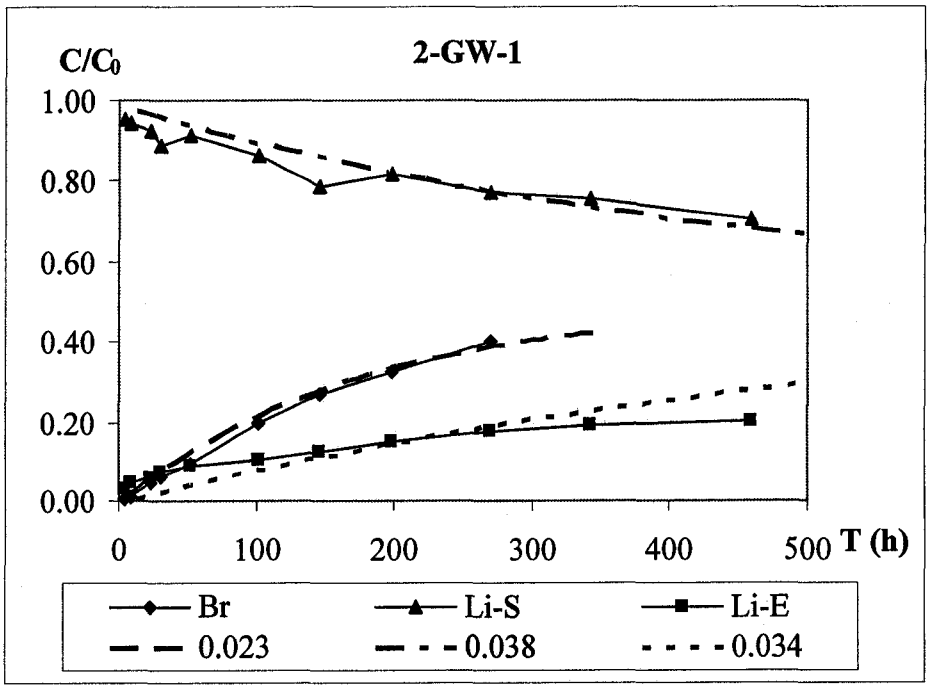

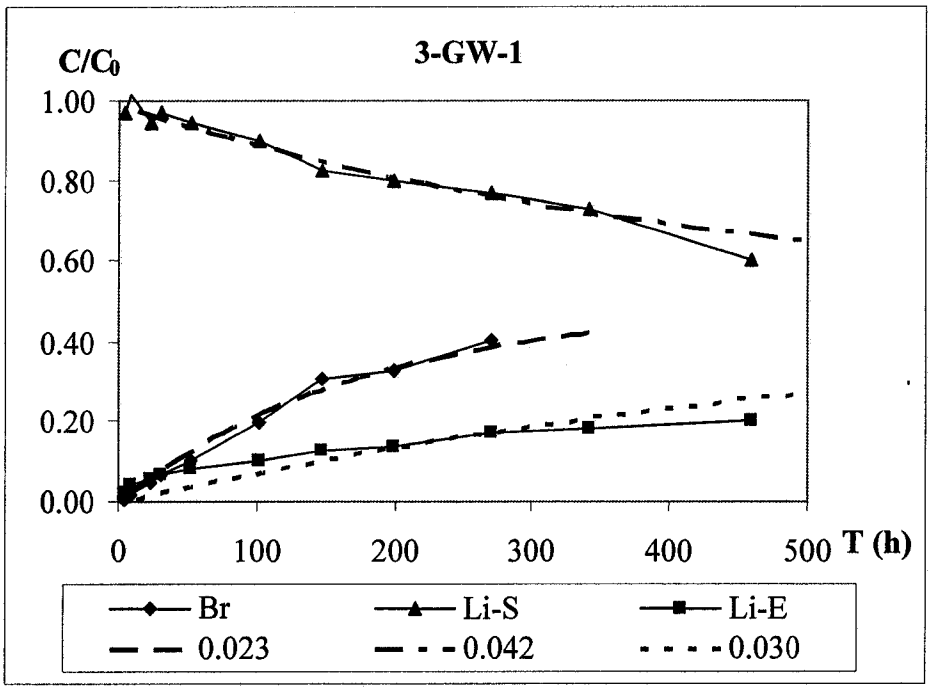

* Numbers presented in the legend of each plot indicate the tortuosity value that gave the best model fit to the corresponding experimental data.

Appendix E: Statistical analysis of the results

Tortuosity results were statistically analyzed for the equality of the population means. Results obtained from Br^- profiles in control cells were compared to those from the biofilm-containing cells for equality of the population means. Tortuosity data for *E. coli* and *P. putida* cells estimated from the Lissamine profiles in the source and exit reservoirs were also analyzed.

Comparisons of statistical significance were performed using a two-sample-two-tailed t-test assuming equal variances and 95% confidence interval. These tests were implemented using canned functions in an MS Excel spreadsheet.

Table E1: t-Test: Control vs. *E. coli*, Br^- concentration data from exit reservoirs

	Control	*Ecoli*
Mean	0.02075	0.0218
Variance	6.92E-06	0.0000012
Observations	4	5
Pooled Variance	3.65E-06	
Degree of Freedom	7	
t Stat	-0.81929	
$P(T \leq t)$ two-tail	0.439621	
t Critical two-tail	2.364624	

Table E2: t-Test: Control vs. *P. putida*, Br^- concentration data from exit reservoirs

	Control	*Pputida*
Mean	0.02075	0.0232
Variance	6.92E-06	7.17E-05
Observations	4	5
Pooled Variance	4.39E-05	
Degree of Freedom	7	
t Stat	-0.551	
$P(T \leq t)$ two-tail	0.598772	
t Critical two-tail	2.364624	

Table E3: t-Test: Control vs. GW, Br^- concentration data from exit reservoirs

	Control	*GW*
Mean	0.02075	0.023
Variance	6.92E-06	1.806E-05
Observations	4	3
Pooled Variance	4.15E-06	
Degree of Freedom	5	
t Stat	-1.44611	
$P(T \leq t)$ two-tail	0.207782	
t Critical two-tail	2.570582	

Table E4: t-Test: *E. coli* vs. *P. putida*, Lissamine concentration data from exit reservoirs

	Ecoli	*Pputida*
Mean	0.028	0.0296
Variance	8E-07	1.68E-06
Observations	5	5
Pooled Variance	1.24E-06	
Degree of Freedom	8	
t Stat	-0.71842	
$P(T \leq t)$ two-tail	0.492943	
t Critical two-tail	2.306004	

Table E5: t-Test: *E. coli* vs. *P. putida*, Lissamine concentration data from source reservoirs

	Ecoli	*Pputida*
Mean	0.046	0.0504
Variance	2.7E-05	6.808E-05
Observations	5	5
Pooled Variance	4.75E-05	
Degree of Freedom	8	
t Stat	-0.31908	
$P(T \leq t)$ two-tail	0.757842	
t Critical two-tail	2.306004	

Appendix F: Calibration of the bromide electrode

Br^- concentration data were detected using a combination bromide electrode (Orion 9635, Thermo Electron Corporation, MA, USA) connected to a millivoltmeter. The readings were obtained in millivolt and an exponential equation, as indicated in the manufacturer's manual, was used to convert the readings in millivolt to Br^- concentration. The electrode was required to be calibrated before each reading.

Br^- standard solutions of 5, 10, 50, 100, 500, and 1000 ppm were prepared using minimal salt solution (to account for any possible interference of other ions) by serial dilution. An exponential curve was fit to the millivolt readings in MS Excel in order to obtain the calibration curve. A sample millivolt reading of standard solution and the corresponding calibration curve are presented in Table F1 and Figure F1 respectively.

Table E1: A sample calibration data

Standard solution concentration (ppm)	Reading (millivolt)
5	73.7
10	78.6
50	177.9
100	135.6
500	176.2
1000	195.0

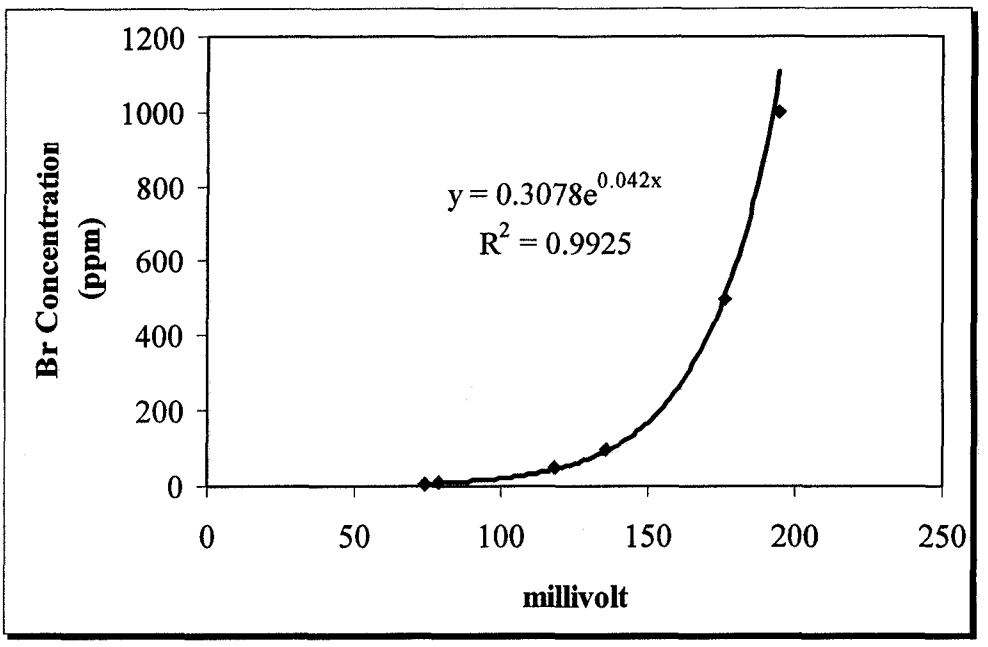

Figure F1: Sample bromide electrode calibration curve